Simple Robust Hedging with Nearby Contracts

Liuren Wu

Zicklin School of Business, Baruch College

Jingyi Zhu

University of Utah

Abstract

Most existing hedging approaches are based on neutralizing risk exposures defined under a pre-specified model. This paper proposes a new, simple, and robust hedging approach based on the affinity of the derivative contracts. As a result, the strategy does not depend on assumptions on the underlying risk dynamics. Simulation analysis under commonly proposed security price dynamics shows that the hedging performance of our methodology based on a static position of three options compares favorably against the dynamic delta hedging strategy with daily rebalancing. A historical hedging exercise on S&P 500 index option further highlights the superior performance of our strategy.

JEL Classification: E43, E47, G10, G12, C51.

Keywords: options, static hedging, forward partial differential equation, local volatility.

We thank Peter Carr, Tom Hurd, and seminar participants at McMaster University and Worcester Polytechnic Institute for discussions and comments. We welcome comments, including references we have inadvertently overlooked. liuren.wu@baruch.cuny.edu (Wu) and zhu@math.utah.edu (Zhu).

Give me a lever long enough and a fulcrum on which to place it, and I shall move the world.

— Archimedes, Mathematician and inventor of ancient Greece, 287-212BC

1. Introduction

In hedging derivatives risk, many think like Archimedes, by making strong, idealistic assumptions on both the security dynamics and the trading environment. For example, Black and Scholes (1973) and Merton (1973) introduce the concept of dynamic hedging by assuming that the underlying security follows a one-factor diffusion process and that one can rebalance the hedge portfolio continuously without incurring any transaction cost. Since then, the idea of dynamic hedging has been extended to multi-factor continuous dynamics based on continuous rebalancing of a portfolio that includes both the underlying security and a finite number of derivative securities. The hedging ratios depend on the particular assumptions on the underlying dynamics. Carr and Wu (2002) propose a static hedging strategy on vanilla options by assuming that the underlying security follows a one-factor Markovian process and that one can deploy an infinite number of short-term options across the whole continuum of strikes.

In reality, transaction cost is a fact of life, under which both continuous rebalancing and transacting on a continuum of options lead to immediate financial ruin. One must therefore discretize the rebalancing frequency under the dynamic hedging approach and discretize the strike continuum under the static hedging application to balance hedging errors with transaction costs.[1] Even more problematic, however, is the fact that one does not know the exact dynamics of the underlying security and thus cannot fully quantify the exposures to each risk source. To the extent that the model is misspecified, hedging errors can result from either mis-calculating the hedging ratios or missing some risk sources all together. For example, most dynamic hedging approaches leave the risk of discontinuous price movements of random sizes unhedged. Furthermore, both the dynamic delta hedging under the Black-Merton-Scholes (BMS) model and the static hedging strategy proposed by Carr and Wu (2002) leave volatility risks unhedged.

[1] Under the Black-Merton-Scholes model environment, the dependence of the delta hedging error on the discretization step has been studied extensively in, for example, Boyle and Emanuel (1980), Bhattacharya (1980), Figlewski (1989), Galai (1983), Leland (1985), and Toft (1996).

Practitioners often perform various ad hoc adjustments to bridge the gap between idealistic theories and reality. For example, due to transaction cost, continuous rebalancing is often reduced to rebalancing daily for stock price exposures and opportunistically for volatility exposures. Furthermore, due to uncertainty in the underlying dynamics, risk exposures are often computed using the Black-Merton-Scholes (BMS) model, but risks are managed far beyond the delta risk, even though delta risk is the only risk source under the BMS model. The vega of the derivative portfolio, i.e., the portfolio's exposure to volatility risk, is also closely monitored and managed. In addition, vega risks at different segments of the implied volatility surface are often managed separately, implicitly recognizing that volatility risk may have multiple dimensions of variation that can affect different segments of the implied volatility surface differently.[2] Such practices may seem inconsistent with the underlying models used for computing the risk exposures, but they provide a simple, albeit primitive, mechanism to defend against model uncertainty and against shocks from possibly multiple, unmodeled risk sources.

In the presence of such uncertainties, the safest way to hedge the risk of a derivative position is to use nearby, similar contracts, which share similar risk characteristics regardless of the underlying dynamics, rather than using vastly different contracts while relying on a model to compute the risk exposure and the hedging ratio. In this paper, we formalize this intuitive idea and derive a hedging strategy not based on risk exposures defined in a model, but based on similarities in observable contract characteristics. To make our idea operational, we focus on European options on the same underlying security and define contract similarities based on their distance in strike and time to maturity.

We start with a short position in a target option contract, and propose to hedge the target position with three nearby option contracts. One can in theory choose more option contracts to form a more accurate hedge portfolio, but transaction cost concerns motivate us to focus on a small number. The strikes and maturities of the three hedging options can be flexibly chosen to balance between contract availability, transaction cost, and hedging effectiveness. We focus on a strike-maturity triangle formulation in which a center strike is placed at one maturity and two outside strikes are placed at another maturity. We perform Taylor series

[2] As a concrete example, a long five-year straddle might be neutralized by a short four-year straddle, but may not be neutralized by a one-month straddle position. Vegas at different segments of the implied volatility surface are often regarded as exposures to different risk sources.

expansions on both the target and the hedging options along the strike and maturity dimension around a common strike and maturity reference point, and we choose the hedging portfolio weights to match the different expansion terms in the target option and the hedging portfolio.

The simple maturity-strike triangle becomes a very effective hedge of the target option for several reasons. First, we Taylor expand along the strike dimension to the second order, and we link the second-order strike derivative (butterfly spreads) to the first-order maturity derivative (calendar spreads) via the local volatility definition of Dupire (1994). While Dupire first proposes the concept of local volatility in a one-factor diffusion setting, the notion of local volatility is well-defined under a much more general setting. Rather than regarding it as a model assumption, we use the local volatility to define the empirically observed relation between butterfly spreads and calendar spreads, without assuming anything about the underlying price dynamics. Through this linkage, we are able to achieve second-order accuracy with merely three options to match coefficients on three terms: the option value, the first strike derivative, and the first maturity derivative at the reference strike and maturity point.

Second, we show that our portfolio formulation allows a partial cancelation of the higher-order terms in the Taylor expansions of the target and hedge options, thus making the hedging errors smaller than the expansion errors of each target or hedge option. Furthermore, when multiple strikes are available, we can match higher-order terms between the target option and the triangle hedge portfolio through appropriate choice of the strike choice for the hedge triangle.

Most importantly, the formulation of our hedging portfolio is completely independent of any assumptions on the underlying risk dynamics. We choose the hedging option maturities and strikes to balance contract availability, transaction cost, and hedging effectiveness, and we derive the hedging portfolio weights based on observed option prices, from which we estimate a local volatility at the reference strike and maturity point, while making no assumptions on the underlying risk dynamics and/or the risk exposures of each contract.

Through extensive Monte Carlo analysis on commonly used stock price dynamics, we show that our static hedge portfolio with three options can perform much better than dynamic hedge with the underlying

futures in all model environments. The simulation exercise also illustrates how one can choose the maturity and strike spacing for the hedging portfolio to further reduce hedging errors. Applying the strategy to S&P 500 index options in a historical test also shows that we can form many maturity-strike triangles from the available option contracts that outperform delta hedging with daily rebalancing. Thus, under practical scenarios, the triangle is simple and flexible for actual implementation, and robust to dynamics variations.

The option pricing literature mostly starts with a fundamental backward partial differential equation (PDE), which defines the value of a derivative contract based on the relations between the exposures of the contract to various risk sources. For example, under the Black-Scholes-Merton model and assuming zero rates, the theta (time derivative) of an option is linearly related to the delta (stock price derivative) and dollar gamma (second stock price derivative) of the option. In the presence of stochastic volatility, vega (volatility derivative), vanna (cross derivative of volatility and price), and volga (second volatility derivative) also come into the backward PDE. Such backward equations define how the risk sensitivities of the derivative contracts link to each other and form the basis for risk-exposure-based hedging approaches. By contrast, our hedging result is built on the forward PDE that relates option derivatives against maturities and strike prices. By exploiting the forward equation, we can match more terms with fewer options. Even if the dynamics underlying the original forward PDE of Dupire (1994) does not hold, we can still use it as a definition for local volatility, through which the maturity derivative and second-strike derivative are linked. To the extend this linkage (and hence the local volatility) is stable over time, better static hedging performance can be achieved by matching second-order strike derivatives.

Since we kept our portfolio weights fixed over the life of the hedging exercise, our hedging approach is the most closely related to the static hedging proposed by Carr and Wu (2002), who use a continuum of short-term options to completely span the risk of a long-term option under the assumption of a one-factor Markovian setting. Since using a continuum of options is not feasible in practice, they also propose a quadrature method to approximate the continuum with a small number of options. We show that their three-strike approximation coincides with a degenerate special case of our maturity-strike triangle, in which all three options in the hedge portfolio lie on one maturity.

In other related literature, the effective hedging of derivative securities has been applied not only for risk management, but also for option valuation and model verification (Bates (2003)). Bakshi, Cao, and Chen (1997), Bakshi and Kapadia (2003), and Dumas, Fleming, and Whaley (1998) use hedging performance to test different option pricing models. Kennedy, Forsyth, and Vetzal (2006) and Kennedy, Forsyth, and Vetzal (2009) sets up a dynamic programming problem in minimizing the hedging errors under jump diffusion frameworks and in the presence of transaction cost. The idea of static spanning, on the other hand, started with the classic works by Breeden and Litzenberger (1978), Ross (1976), Green and Jarrow (1987), and Nachman (1988). These authors show that a path-independent payoff can be hedged using a portfolio of standard options maturing with the claim. More recently, Carr and Chou (1997) considers the static hedging of barrier options and Carr and Madan (1998) proposes a static spanning relation for a general payoff function by a portfolio of bond, forward, European options maturing at the same maturity with the payoff function. Starting with such a spanning relation, Takahashi and Yamazaki (2009a,b) propose a static hedging relation for a target instrument that has a known value function.

The remainder of the paper is organized as follows. The next section defines the hedging procedure, and derives the optimal weights for the maturity-strike triangle hedging portfolio. Section 3 provides a numerical study on the effectiveness of the hedging strategy and how the effectiveness varies across different maturity combinations and strike spacing choices. Section 4 applies the hedging strategy to a long history of S&P 500 index options. Section 5 concludes.

2. A New Theoretical Framework for Hedging with Nearby Contracts

To make the idea concrete, we start at time t with a unit short position in a European call option with strike K and expiry T, and we consider hedging this option position by using a small number (three, to be exact) of European call options at nearby strikes and maturities. When necessary, put-call parity can be applied to switch call options to put options. In the absence of transaction cost, one can in principle form a hedge portfolio with more options to achieve better hedging performance; nevertheless, practical transaction cost concerns motivate us to limit to three options in forming the hedge portfolio.

2.1. Assumptions and notations

We use $C(K,T)$ to denote the time-t value of a call option at strike K and expiry T. To avoid notational clustering, we assume zero rates and suppress the dependence of the call option value on calendar time t, the spot price S, and other potential risk sources, as long as no confusion shall occur.

Given observed option prices across different strikes and maturities, we define the local volatility surface, $\sigma(K,T)$, via the Dupire (1994) equation in terms of the partial derivatives of the option values against strike and maturity,

$$\sigma^2(K,T) \equiv \frac{2C_T(K,T)}{K^2 C_{KK}(K,T)}, \tag{1}$$

where C_T denotes the first partial derivative of the call option value with respect to maturity and C_{KK} denotes the second partial derivative with respect to strike. Dupire first derives the forward PDE in a one-factor diffusion setting; however, the notion of local volatility as defined in equation (1) is well-posed under a much more general setting. In particular, the existence of a positive and finite local volatility surface can be used as a condition to exclude arbitrage opportunities.

In practice, only a finite number of option prices are observable across a discrete number of strikes and maturities. Thus, one needs to perform interpolation and extrapolation over the finite observations to evaluate the maturity and strike derivatives to arrive at the local volatility estimates. When options are quoted in BMS implied volatilities, one can also compute the local volatility directly from the interpolated implied volatility surface, e.g., Coleman, Li, and Verma (1998), Lee (2005), and Gatheral (2006). We assume that one can perform reasonably stable interpolation and extrapolation on observed option prices or implied volatilities to obtain finite and positive estimates of local volatilities at strikes and maturities of interest. We make no assumptions on the underlying security price or volatility dynamics.

2.2. Hedging with a maturity-strike triangle triangle

We propose a strategy to hedge the risk of the target option $C(K,T)$ with three nearby options. In principle, the three option contracts can all have different strikes and maturities. Since often fewer maturities are

available in practice, we focus on a **maturity-strike triangle** formulation, where the three options have three different strikes $K_d < K_c < K_u$ but two different maturities, with the center strike K_c at one maturity T_c and the two outside strikes (K_d, K_u) at another maturity T_o. There is no particular restriction on the order of the three maturities T_c, T_o, T, but practically it is likely that one chooses more liquid shorter-term options to hedge the possibly less liquid longer-term option, that is, $T_c, T_o < T$. Furthermore, it is natural to choose the hedge option strikes around the target option strike $K_d < K < K_u$, with possibly $K_c = K$ when K is available at T_c.

The hedging strategy that we propose does not rely on matching the risk exposures of the hedging portfolio with that of the target option because risk exposure calculations depend on the particular specification of the underlying security price and volatility dynamics. Instead, our strategy is based on the affinity of the triangle hedge portfolio to the target option in terms of their strikes and maturities.

Given the layout of the maturity-strike triangle, we derive the hedge portfolio weights through the following procedure. First, we perform Taylor expansions on both the target option and the hedge portfolio along the maturity and strike dimensions around a common reference point, (K, T_o),

$$
\begin{aligned}
C(K,T) &\approx C(K,T_o) + C_T(K,T_o)(T - T_o), && (2)\\
C(K_d,T_o) &\approx C(K,T_o) + C_K(K,T_o)(K_d - K) + \frac{1}{2}C_{KK}(K,T_o)(K_d - K)^2, && (3)\\
C(K_u,T_o) &\approx C(K,T_o) + C_K(K,T_o)(K_u - K) + \frac{1}{2}C_{KK}(K,T_o)(K_u - K)^2, && (4)\\
C(K_c,T_c) &\approx C(K,T_o) + C_K(K,T_o)(K_c - K) + C_T(K,T_o)(T_c - T_o) + \frac{1}{2}C_{KK}(K,T_o)(K_c - K)^2. && (5)
\end{aligned}
$$

We expand the options along the maturity dimension to the first order and along the strike dimension to the second order. The expansion generate four terms $C(K,T_o)$, $C_K(K,T_o)$, $C_{KK}(K,T_o)$, and $C_T(K,T_o)$. Unfortunately, we cannot use a portfolio of three options to match four expansion terms. Fortunately, we can replace the second strike derivative $C_{KK}(K,T_o)$ with the first maturity derivative $C_T(K,T_o)$ via the local volatility definition in equation (1),

$$
C_{KK}(K,T_o) = \frac{2}{\sigma(K,T_o)^2 K^2} C_T(K,T_o). \qquad (6)
$$

With this replacement, we can choose the portfolio weights (w_d, w_c, w_u) for the three options at strikes (K_d, K_c, K_u) to match the coefficients on the three terms between the target option expansion and the hedge portfolio expansion: the option value $C(K,T_o)$, the first-order strike derivative $C_K(K,T_o)$, and the first-order maturity derivative $C(T(K,T_o)$.

Matching the coefficients on $C(K,T_o)$, we have

$$1 = w_d + w_u + w_c, \tag{7}$$

which says that the sum of the hedge portfolio weights is equal to the target option weight. Matching the coefficients on $C_K(K,T_o)$, we have,

$$0 = w_d(K_d - K) + w_u(K_u - K) + w_c(K_c - K). \tag{8}$$

Plugging the weight condition in (7) to (8), we have,

$$K = w_d K_d + w_u K_u + w_c K_c, \tag{9}$$

which says that the weighted average of the chosen strikes in the hedge portfolio should be equal to the target strike. Finally, matching the coefficients on $C_T(K,T_o)$ and normalizing both sides by $(T - T_o)$, we have

$$1 = \sum_j w_j \frac{(K_j - K)^2}{\sigma^2(K,T_o)K^2(T - T_o)} - w_c \frac{T_o - T_c}{T - T_o}, \quad j = d,u,c. \tag{10}$$

We can solve for the three portfolio weights from the three conditions (7), (9), and (10).

Now, we introduce a standardized measure of strike spacing around the target strike point,

$$d_j \equiv \frac{(K_j - K)}{K\sigma(K,T_o)\sqrt{T - T_o}}, \quad j = d,c,u. \tag{11}$$

Intuitively, the standardized spacing measure d_j approximates the number of standard deviations that the

security price needs to move from (T_o, K_j) to (T, K). We also define a relative maturity spacing measure,

$$\alpha \equiv \frac{T_o - T_c}{T - T_o}, \tag{12}$$

which measures the relative distance between the two maturities in the hedge triangle to the distance between the target option maturity and the reference hedge maturity T_o. The third condition in (10) can be written in terms of the standardized strike spacing d_j and maturity spacing α,

$$1 = w_d d_d^2 + w_u d_u^2 + w_c (d_c^2 - \alpha). \tag{13}$$

The following proposal summarizes the results on the maturity-strike triangle hedge portfolio.

Proposition 1 *To hedge the risk of a target option at (K, T), we propose to form a hedge portfolio with three options forming a maturity-strike triangle, in which the three options are placed at three strikes $K_d < K_c < K_u$) and two maturities with (K_d, K_u) at T_o and K_c at T_c. The portfolio weights can be chosen to match the maturity and strike expansions of the triangle with that of the target option,*

$$\begin{bmatrix} w_d \\ w_c \\ w_u \end{bmatrix} = \begin{bmatrix} 1 & 1 & 1 \\ K_d & K_c & K_u \\ d_d^2 & d_c^2 - \alpha & d_u^2 \end{bmatrix}^{-1} \begin{bmatrix} 1 \\ K \\ 1 \end{bmatrix}. \tag{14}$$

An important observation from the proposition is that the portfolio weights only depend on the relative strike and maturity spacing of the hedge and target options, but do not explicitly depend on the calendar time or the spot price level. In this sense, the hedge portfolio is static. One caveat is that we use the local volatility $\sigma(K, T_o)$ to standardize the strike spacing in (11). To the extent that the local volatility is varying over time, so is the standardized strike spacing for a fixed set of option contracts. The portfolio weights can vary as a result. In application, we assume that the relation between C_T and C_{KK} is stable over time, and treat the hedge portfolio as an approximate, static portfolio.

The proposal imposes little constraints on the strike and maturity choice in the triangle. In what follows, we consider several interesting special cases of the general proposal.

2.2.1. Symmetric triangles

If we place the center strike at the target option strike $K_c = K$ and choose equal spacing for the two outer strikes, $K_u - K = K - K_d$, we obtain a symmetric (isosceles) triangle. In this case, $d_c = 0$ and we let $d = |d_u| = |d_d|$ denotes the standardized equal distance from the two outer strikes to the center. The result becomes particularly simple.

Proposition 2 *When the maturity-strike triangle is symmetric around the target strike, with $K_c = K$ and $K_u - K = K - K_d$, the portfolio weights are given as a function of the standardized strike spacing $d = |d_u| = |d_d|$ and relative maturity distance α,*

$$w_c = \frac{d^2 - 1}{d^2 + \alpha}, \quad w_d = w_u = \frac{1}{2}(1 - w_c). \tag{15}$$

Proof. From the first and second conditions in (7) and (9), we can infer that symmetric strike choice leads to symmetric portfolio weights $w_d = w_u = 1 - w_c$. Plugging in the symmetric weight condition into the third condition in (13), we can solve for the center strike weight as in (15). ■

The isosceles triangle has its peak at maturity T_c and its base at maturity T_o. Depending on the ranking of the three maturities (T_c, T_o, T), the triangle can be formed in a number of ways. For practical considerations, we focus on the cases in which the maturity of the target option T is longer than the maturities (T_o, T_c) of the hedging options in the triangle. With this constraint, the triangle can be formed with either (i) $T_c < T_o < T$ and thus $\alpha > 0$, where the triangle points to the shorter maturity, or (ii) $T_o < T_c < T$ and thus $-1 < \alpha < 0$, where the triangle points to the longer maturity. As the relative maturity distance α takes on different ranges of values in the two cases, the portfolio weights also show different behaviors as a function of the standardized strike spacing d. With positive α in the first case, the portfolio weight on the center strike (w_c) increases monotonically with the strike spacing from $-1/\alpha$ at $d = 0$ to 1 as d approaches infinity. When the

three maturities are equally spaced and hence $\alpha = 1$, the portfolio weight on the center strike varies from -100% to 100% as the strike spacing increases from zero to infinity.

In the second case in which the center strike maturity is longer than the maturity of the outer strikes ($T_o < T_c < T$) and thus the relative maturity distance α becomes negative, the portfolio weight w_c has a singularity at $d^2 + \alpha = 0$. The center strike weight w_c approaches positive infinity as $d^2 \uparrow -\alpha$ and negative infinity as $d^2 \downarrow -\alpha$.

In both cases, as long as the strikes are spaced one standard deviation away ($d > 1$), the portfolio weights on all three points of the triangle are positive, and the weight on the center strike increases with increasing strike spacing for the two outside strikes. Figure 1 plots the center strike weight w_c as a function of the standardized strike spacing d in both cases with the assumption of equal spacing between the three maturities, and thus $\alpha = 1$ for the first case and $\alpha = -1/2$ for the second case. The solid line shows the monotonic and slow increase of the center strike weight from -100% to 100% as a function of the strike spacing d. The dashed line reveals the singularity at $d = \sqrt{1/2}$. When $d > 1$, both cases generate positive weights on the center strike and the two outside strikes.

[Figure 1 about here.]

2.2.2. A degenerating line of three strikes at one maturity

The hedge remains well-defined when the maturity-strike triangle degenerates into a line of three strikes as the two maturities shrink to one $T_o = T_c$. In this case, we label the maturity of the options in the hedging portfolio as T_h. With symmetric strike placement, the portfolio weight on the center strike option increases with strike spacing.

Proposition 3 *When the symmetric maturity-strike triangle degenerates into a line of three strikes symmetrically placed around the target strike, the hedge portfolio weights are reduced to be a function of the*

standardized strike spacing only,

$$w_c = 1 - \frac{1}{d^2}, \quad w_d = w_u = \frac{1}{2}(1 - w_c). \tag{16}$$

When we approximate the target option with three strikes at one maturity T_h, the approximation is analogous to a trinomial tree, and the weight on the center strike increases with the strike spacing. When the outer strikes are about one standard deviation away from the center $d = 1$, the center weight is zero and the trinomial tree degenerates into a binomial tree. When the strikes are spaced more than one standard deviation away, the weights on all three strikes become positive. For example, at two standard deviation strike spacing $d = 2$, the center strike takes a weight of $\frac{3}{4}$, and the weights on the two outer strikes are $\frac{1}{8}$ each. The three strikes take on equal weight of $\frac{1}{3}$ each when the strike spacing is $d = \sqrt{3/2}$.

Under a one-factor Markovian setting, Carr and Wu (2003) (henceforth CW) derives a static hedging strategy for a vanilla option $C(K,T)$ using a continuum of options at at a shorter maturity $T_h < T$. Different from our approximations based on Taylor series expansions, the CW static hedge is an exact relation if (i) the underlying security price dynamics is known, (ii) the security price dynamics is one-factor Markovian, and (iii) a continuum of options are available at a shorter maturity to form the hedging portfolio. However, none of the three conditions are likely to hold in reality. Investors do not know the true underlying price dynamics. The dynamics are unlikely to be one-factor Markovian because stochastic volatilities for most securities, with independent variations, are well-documented. Finally, option contracts are available only at a finite number of strikes. Furthermore, to minimize transaction costs, one can only use a small number of options to form the hedge portfolio. CW propose a discrete-strike implementation procedure in which the strikes and portfolio weights are chosen based on a Gauss-Hermite quadrature approximation of the integral in the theoretical relation. In particular, given the quadrature points and weights (x_j, ω_j) and with zero rates, the strikes and portfolio weights are given as,

$$K_j = K e^{\sqrt{2} x_j \sigma \sqrt{(T-T_h)} - \frac{1}{2}\sigma^2 (T-T_h)}, \quad w_j = \omega_j / \sqrt{\pi}, \tag{17}$$

where σ denotes a volatility estimate for the underlying security return. If we ignore the convexity term and the difference between percentage returns and log returns, our standardized strike spacing measure d_j relates approximately to the quadrature point by $d_j \approx \sqrt{2x_j}$. In the three-strike case, the quadrature points are given as $(0, \pm\sqrt{3/2})$, corresponding to a standardized strike spacing of $d \approx \sqrt{3}$. The quadrature weight for the center point is $\frac{2}{3}\sqrt{\pi}$, corresponding to a portfolio weight for the center strike of $2/3$, exactly the same as implied by equation (16) in our Proposition 3, $w_c = 1 - 1/d^2 = 2/3$. Therefore, the CW three-strike discrete implementation coincides with a very special example of our degenerate case of a line of three strikes, with the strike spacing being pre-set according to the quadrature rule. Our approach is much more general. It allows the allocation of the three strikes at two arbitrary maturities; the strike spacing is not pre-determined, but can be chosen with flexibility to balance contract availability, transaction cost, and hedging performance; and finally, the hedge portfolio formulation is independent of any dynamics assumptions.

2.2.3. A degenerating line of two maturities at one strike

When all three strikes in the hedge portfolio coincide with the target strike $K_u = K_d = K_c = K$, the maturity-strike triangle further degenerates into a line of two contracts at two maturities. If we retain the notation of T_c and T_o, with no particular ranking, the portfolio weights are determined purely by the relative maturity distance α.

Proposition 4 *When the symmetric maturity-strike triangle degenerates into a line of two option contracts at two maturities (T_c, T_o) and the same strike K, the hedge portfolio weights are reduced to a function of the relative maturity spacing α only,*

$$w_c = -\frac{1}{\alpha}, \quad w_o = 1 + \frac{1}{\alpha}. \tag{18}$$

When the target option maturity T is either longer or shorter than both maturities in the hedge portfolio, the portfolio always contains a short position in the shorter maturity and a long, levered position in the longer maturity. On the other hand, if the target option maturity is sandwiched by the two maturities in the hedge portfolio, the portfolio weights are positive for both options.

While our focus is on the maturity-strike triangle, the two degenerate lines illustrate the generality of our proposal as it includes the CW static hedging as a very special case, and it allows investors to trade both the implied volatility smile and the term structure, either together or separately, while managing their risk exposures.

2.3. From expansion errors to hedging errors

Our hedging portfolio weights are derived by matching the corresponding terms in the Taylor expansions of the target option and the hedge portfolio. The expansion error on each option contract increases with the distance between the contract's strike and maturity and the reference strike and maturity expansion point. In practice, strikes are often available at a fine grid, but maturities tend to be more sparse. Thus, the expansion errors along the maturity dimension can be large. However, we show in this section that the expansion error of the hedged portfolio can be much smaller than the average expansion error of the individual contracts due to cancelation. We illustrate this point through two angles. First, we show that although the expansion error on each option contract depends on the reference point around which the expansion is performed, the portfolio weights for the hedge triangle do not explicitly depend on the particular choice of the expansion reference point. Second, we perform the Taylor expansion to a higher order and show how the leading-term expansion error on the target options cancels with the leading-term expansion error on the hedge portfolio. We further show how one can maximize the cancelation via appropriate choice of the strike spacing in the hedge portfolio.

2.3.1. Independence of portfolio weights on the expansion reference point

In deriving our portfolio weights, we expand both the target option and the hedge options around a common strike and maturity reference point (K, T_o). This reference point is a convenient choice because with this reference point, we only need to perform maturity expansion for the target option and the hedge option at the center strike when $K_c = K$, and we only need to perform strike expansion on the two hedge options at the outside strikes. Choosing other expansion points would lead to more terms. However, the following

proposition shows that the particular choice of the reference point is not important for computing the hedge portfolio weights.

Proposition 5 *When the local volatility is flat across strikes and maturities, the portfolio weights do not depend on the reference maturity and strike point, around which the Taylor expansion is performed.*

Proof. Let (K_m, T_m) be an arbitrary strike-maturity reference point, with which we perform the Taylor expansion on the target and hedge options:

$$\begin{aligned}
C(K,T) &\approx C + C_K(K-K_m) + C_T(T-T_m) + \frac{1}{2}C_{KK}(K-K_m)^2, \\
C(K_u,T_o) &\approx C + C_K(K_u-K_m) + C_T(T_o-T_m) + \frac{1}{2}C_{KK}(K_o-K_m)^2, \\
C(K_u,T_o) &\approx C + C_K(K_d-K_m) + C_T(T_o-T_m) + \frac{1}{2}C_{KK}(K_o-K_m)^2, \\
C(K_c,T_c) &\approx C + C_K(K_c-K_m) + C_T(T_c-T_m) + \frac{1}{2}C_{KK}(K_c-K_m)^2,
\end{aligned}$$

where the term C, C_K, C_T, and C_{KK} are all evaluated at the reference point (K_m, T_m) and we hide the dependence to reduce notation clustering. Matching the option level C term, we have $1 = w_u + w_d + w_c$ as before. Matching the C_K term, we have

$$(K-K_m) = w_u(K_u-K_m) + w_d(K_d-K_m) + w_c(K_c-K_m), \tag{19}$$

which in combination with the first condition leads to,

$$K = w_u K_u + w_d K_d + w_c K_c. \tag{20}$$

Thus, neither the first nor the second condition depends on the reference point choice (K_m, T_m).

Matching the C_T and C_{KK} term, we have

$$C_T(T-T_m) + \frac{1}{2}C_{KK}(K-K_m)^2 = \sum_j w_j C_T(T_j-T_m) + \frac{1}{2}C_{KK}(K_j-K_m)^2, \tag{21}$$

with $j = u, d, c$. We see that the T_m terms cancel out. Furthermore, if we write $K_j - K_m = (K_j - K) + (K - K_m)$ and expand the $(K_j - K_m)^2$ terms, the condition in (21) simplifies to

$$C_T T = \sum_j w_j C_T T_j + \frac{1}{2} C_{KK} (K_j - K)^2, \tag{22}$$

which does not has any explicit dependence on the reference point (K_m, T_m). Therefore, the portfolio weights do not have explicit dependence on the reference point for the Taylor expansion.

An implicit dependence arise when we convert C_{KK} into C_T via the local volatility definition. Since the local volatility is evaluated at the reference point (K_m, T_m), portfolio weights depend on the reference point to the extent that the local volatility is strike and maturity dependent. When the local volatility surface is flat, the portfolio weights are completely independent of the reference point choice. ■

The expansion error on each option contract depends obviously on the reference point. The closer the reference point is to the strike and maturity of the contract, the smaller the expansion error is. Yet, the above proposition shows that the hedge portfolio weights are quite robust with respect to the reference point choice. In particular, with a flat local volatility surface, the portfolio weights and hence the hedging errors are independent of the reference point that we choose for the expansion.

2.3.2. Leading-term expansion errors in target and hedge options

To analyze how the expansion errors cancel between target and hedge options, we expand each option contract to a higher order and analyze the behavior of the leading-term expansion error. To reduce notation clustering, we use (K, T_o) as the reference point for the expansion, we hide the explicit dependence on the reference point in the notation, and we focus on the symmetric maturity-strike triangle for the analysis, with

$\Delta K = K_u - K = K - K_d$ and $\Delta T = T - T_o$. The expansions become,

$$\begin{aligned}
C(K,T) &\approx C + C_T \Delta T + \frac{1}{2} C_{TT} (\Delta T)^2, && (23)\\
C(K_u,T_o) &\approx C + C_K \Delta K + \frac{1}{2} C_{KK} (\Delta K)^2 + \frac{1}{6} C_{KKK} (\Delta K)^3 + \frac{1}{24} C_{KKKK} (\Delta K)^4, && (24)\\
C(K_d,T_o) &\approx C - C_K \Delta K + \frac{1}{2} C_{KK} (\Delta K)^2 - \frac{1}{6} C_{KKK} (\Delta K)^3 + \frac{1}{24} C_{KKKK} (\Delta K)^4, && (25)\\
C(K,T_c) &\approx C - C_T \alpha \Delta T + \frac{1}{2} C_{TT} \alpha^2 (\Delta T)^2. && (26)
\end{aligned}$$

From the above expansions, we can see that when $\Delta K = 0$, the leading-term expansion error in the target option is $\frac{1}{2} C_{TT} (\Delta T)^2$, which partially cancels with the leading-term expansion error in the hedge portfolio, $w_c \alpha^2 \frac{1}{2} C_{TT} (\Delta T)^2$, when the portfolio weight on the center strike is positive.

When $\Delta K > 0$, additional expansion errors are introduced in the hedge portfolio in terms of the C_{KKKK} term. These additional expansion errors can be used to further cancel out the errors on the C_{TT} terms. To link these higher-order terms, we further differentiate the forward PDE with respective to T,

$$\begin{aligned}
C_{TT} &= \tfrac{1}{2}\sigma^2 K^2 (C_T)_{KK} + \tfrac{1}{2}\sigma_T^2 K^2 C_{KK},\\
&= \tfrac{1}{4}\sigma^4 K^4 C_{KKKK} + \left(\tfrac{1}{2}\sigma^2\sigma_K^2 K^4 + \sigma^4 K^3\right) C_{KKK}\\
&\quad + \left(\tfrac{1}{2}\left(\sigma^4 + \sigma_T^2\right) K^2 + \sigma^2\sigma_K^2 K^3 + \tfrac{1}{4}\sigma^2\sigma_{KK} K^4\right) C_{KK}, \qquad (27)
\end{aligned}$$

where σ_T^2, σ_K^2, and σ_{KK}^2 denote the partial derivatives of the local variance σ^2, which are all zero in the case of a flat local volatility surface. To remove the C_{KKK} term in equation (27), we assume that $S = K$ and link C_{KKK} to C_{KK} according to the BMS model, $C_{KKK} \approx -\frac{3}{2}\frac{C_{KK}}{K}$. Then, we have

$$C_{TT} \approx a_2 C_{KK} + \frac{1}{4}\sigma^4 K^4 C_{KKKK}, \qquad (28)$$

with $a_2 = \left(\frac{1}{2}\sigma_T^2 - \sigma^4\right) K^2 + \frac{1}{4}\sigma^2\sigma_K^2 K^3 + \frac{1}{4}\sigma^2\sigma_{KK}^2 K^4$.

Now, we can use the forward PDE and equation (28) to convert the C_T and C_{TT} terms in the expansions

(23) to (26) to C_{KK} and C_{KKKK} terms,

$$\begin{aligned}
C(K,T) &\approx C+\frac{1}{2}\sigma^2K^2C_{KK}\Delta T+\frac{1}{2}a_2C_{KK}+\frac{1}{8}\sigma^4K^4C_{KKKK}(\Delta T)^2, && (29)\\
C(K_u,T_o) &\approx C+C_K\Delta K+\frac{1}{2}C_{KK}(\Delta K)^2+\frac{1}{6}C_{KKK}(\Delta K)^3+\frac{1}{24}C_{KKKK}(\Delta K)^4, && (30)\\
C(K_d,T_o) &\approx C-C_K\Delta K+\frac{1}{2}C_{KK}(\Delta K)^2-\frac{1}{6}C_{KKK}(\Delta K)^3+\frac{1}{24}C_{KKKK}(\Delta K)^4, && (31)\\
C(K,T_c) &\approx C-\alpha\frac{1}{2}\sigma^2K^2C_{KK}(\Delta T)+\frac{1}{2}a_2C_{KK}+\alpha^2\frac{1}{8}\sigma^4K^4C_{KKKK}(\Delta T)^2. && (32)
\end{aligned}$$

The terms on C and C_K remain the same as before, from which we obtain $w_u+w_d+w_c=1$ and $w_u=w_d=(1-w_c)/2$. Matching the C_{KK} terms, we have,

$$1+\frac{a_2\Delta T}{\sigma^2K^2}=(1-w_c)d^2-\alpha w_c\left(1-\alpha\frac{a_2}{\sigma^2K^2}\Delta T\right),$$

from which we can solve for w_c,

$$w_c=\frac{d^2-1+h}{d^2+\alpha+\sigma^2h}, \tag{33}$$

where

$$h=-\frac{a_2}{\sigma^2K^2}\Delta T=\left(\sigma^4-\frac{1}{2}\frac{\sigma_T^2}{\sigma^2}-\frac{1}{4}\sigma_K^2K-\frac{1}{4}\sigma_{KK}^2K^2\right)\Delta T, \tag{34}$$

which is a function of the local volatility level, its slope along the term structure and strike dimension, its curvature along the strike dimension, and the maturity-distance between the target option and the hedge options for the two outside strikes. Thus, by matching higher-order terms, the portfolio weights are modified by the higher-order term h. When the local volatility is flat across strike and maturity, $h=\sigma^4T$ becomes a very small term and can be safely ignored. When the local volatility surface is heavily skewed across strike or is having a steep term structure, the adjustment can become significant.

Finally, if we are free to choose the strike spacing, we can also match the higher-order term C_{KKKK} term by setting,

$$w_c=\frac{d^4-3}{d^4-3\alpha^2}. \tag{35}$$

Combining (33) and (35), we can solve the standardized strike spacing that matches the higher-order term,

$$d^2 = \frac{3}{2(1-h(1-\alpha))}\left(1-\alpha+\sqrt{(1-\alpha)^2+\frac{4}{3}\alpha(1-h(1-\alpha))}\right), \tag{36}$$

which is a function of the relative maturity spacing α and the term h, which is proportional to the maturity spacing ΔT.

When we ignore the higher-order term h and set $\alpha = 0$ and hence all three strikes in the hedge portfolio fall on the same maturity, we have $d^2 = 3$, the same as the result from the Hermite-Gauss quadrature approximation in Carr and Wu (2002). Therefore, in the sense of matching leading-term expansion errors, the quadrature strike choice is optimal. On the other hand, when the three maturities are equally spaced $T - T_o = T_o - T_c$ and hence $\alpha = 1$, we have $d^2 = \sqrt{3}$.

It is important to realize that the optimal strike spacing in (36) is derived under strong assumptions to remove the C_{KKK} term, and thus shall not be taken literally. Nevertheless, the derivation shows the potential of further reducing the hedging error by appropriate strike spacing choice.

To show the prospect of the expansion error cancelation, Figure 2 plots the leading-term expansion error of the hedged portfolio as a function of the standardized strike spacing measure d. The plots are computed from the Black-Scholes model with $\sigma = 0.25$, zero rates, and with the maturity choices (T_c, T_o, T) being one, two, and six months, respectively. The three lines represent three different target option strikes at $K = \$90$ (dashed line), \$100 (solid line), and \$110 (dash-dotted line), relative to a normalized spot price level of \$100. The plots highlight the prospect of choosing strike spacing judiciously to eliminate the leading-term expansion errors of the hedged portfolio.

[Figure 2 about here.]

3. Numerical Experiments Based on Commonly Specified Dynamics

We gauge the performance of our proposed hedging strategy under several commonly specified security price dynamics. First, we analyze how the strike spacing choice affects the hedging performance under each strategy. Then, we compare the hedging performance of the different strategies with one another and with daily delta hedging with the underlying futures.

3.1. Data-generating processes

We consider four data generating processes: the Black-Scholes model (BS), the Merton (1976) jump-diffusion model (MJ), the Heston (1993) stochastic volatility model (HV), and the jump-diffusion stochastic volatility model of Huang and Wu (2004) (HW). The time-series stock price dynamics are governed by the following stochastic differential equations,

$$\begin{aligned}
\text{BS:}\quad dS_t/S_t &= \mu dt + \sigma dW_t, \\
\text{MJ:}\quad dS_t/S_t &= \mu dt + \sigma dW_t + \textstyle\int_{\mathbb{R}^0} (e^x - 1)\left(\nu(dx,dt) - \lambda n(x) dx dt\right), \quad n(x) = \frac{1}{\sqrt{2\pi\nu_j}} \exp\left(-\frac{(x-\mu_j)^2}{2\nu_j}\right), \\
\text{HV:}\quad dS_t/S_t &= \mu dt + \sqrt{v_t} dW_t, \\
\text{HW:}\quad dS_t/S_t &= \mu dt + \sqrt{v_t} dW_t + \textstyle\int_{\mathbb{R}^0} \left(\nu(dx,dt) - v_t \lambda_0 n(x) dx dt\right), \\
dv_t &= \kappa(\theta - v_t)\, dt - \omega\sqrt{v_t} dZ_t, \quad \mathbb{E}\left[dZ_t dW_t\right] = \rho dt,
\end{aligned} \tag{37}$$

where W_t denotes a standard Brownian motion in all four models. The MJ model also incorporates a compound Poisson jump component, where we use $\nu(dx,dt)$ to denote the counting measure for the jumps, $\mathbb{R}^0$ to denote the real line excluding zero, and $\lambda n(x) dx dt$ to be the compensator, with λ measuring the mean jump intensity or arrival rate, $n(x)$ denotes a normal probability density function capturing the jump size distribution in log return conditional on a jump occurring. Under the Heston (HV) model, Z_t denotes another standard Brownian motion that governs the randomness of the instantaneous variance rate. The two Brownian motions have an instantaneous correlation of ρ. The HW model combines HV with MJ and allows the jump arrival rate to be proportional to the instantaneous variance rate, $\lambda_t = \lambda_0 v_t$. The HW model is labeled as MJDSV3 in Huang and Wu (2004), who show that the model performs better in pricing S&P

500 index options than does a similar model with constant jump arrival rate proposed by Bates (1996) and Bakshi, Cao, and Chen (1997).

The four processes are carefully chosen for our analysis. The BS and MJ models serve as static pure diffusion and jump-diffusion benchmarks, respectively, whereas the HV and HW models allow stochastic volatility for the two benchmarks. Option prices under the BS model can be readily computed using the analytical Black-Scholes option pricing formula. Under the MJ model, option prices can be computed as a Poisson-probability weighted sum of the Black-Scholes formulae. For HV and HW, option prices are computed numerically through fast Fourier inversion of the analytical return characteristic function.

To simulate the data-generating processes and price options on each simulated path, we need to choose appropriate values for the model parameters. To make the analysis comparable to our historical analysis on the S&P 500 index (SPX) options in the next section, we set the parameter values to those calibrated to the SPX options market. Specifically, we perform daily calibration of the HV model and the HW model on SPX options from January 1996 to March 2009, and use the sample averages of the daily parameter estimates for the simulation analysis. The parameters for the BS model and the MJ model are adopted directly from the corresponding parameters from the HV and HW models, respectively, with the constant volatility level set to its long-run mean estimate. Table 1 reports the parameter values used in our analysis. Estimating the HV model generates an average long-run mean volatility of $\sqrt{\theta} = 22.77\%$, an average instantaneous volatility rate level of $\sqrt{v_t} = 18.64\%$. The difference between the two implies an average upward sloping implied volatility term structure. The average mean-reversion coefficient is at $\kappa = 3.7863$, corresponding roughly to quarterly frequency $(1/\kappa)$. The average volatility of volatility coefficient estimate is quite large at $\omega = 0.9095$, which contributes to the curvature of the implied volatility smile. Finally, the average correlation between return and return variance is strongly negative at $\rho = -0.6824$, consistent with the strongly negatively skew observed in the implied volatility smile on SPX options.

By adding a jump component in the HW model, the average long-run mean volatility of the diffusion component becomes lower at $\sqrt{\theta} = 18.69\%$ because the jump component also contributes to the total volatility level, which is at $\sqrt{\theta(1+\lambda_0(\mu_j^2+\sigma_j^2))} = 22.44\%$, very close to the HV estimate. The average

jump frequency is $\lambda_0\theta = 0.4995$, about one jump every two years. Conditional on a jump occurring, the average jump size in return is $\mu_j = -10.21\%$, with a standard deviation of $\sigma_j = 14.32\%$. The large negative jump size contributes to short-term implied volatility skews in the SPX options, and the jump size uncertainty (σ_j) adds curvature to the skew. With the jump component, both the mean-reversion coefficient and the volatility of volatility coefficient average lower at $\kappa = 1.8766$ and $\omega = 0.3811$, respectively. The return-volatility correlation remains strongly negative at $\rho = -0.7564$.

The daily calibration on SPX options generates parameter estimates under the risk-neutral measure. To obtain the corresponding values for the statistical process, we assume zero risk premiums by setting $\mu = r - q$, and use the same set of parameters both for simulating the sample paths and for option pricing. During this sample period, the S&P 500 index started at 617.7, went over 1500 in year 2000 and 2007, but ended the sample at 822.92. The average ex-dividend return on the index over the sample period is 2.17%. The interest rates (r) and dividend yields (q) underlying the option contracts average at 4.17% and 2.58%, which we use as constants for the simulation and option pricing.

3.2. Monte Carlo procedures

In each simulation, we generate a time series of daily underlying security prices according to an Euler approximation of the respective data generating process. The starting value for the stock price is normalized to \$100, and the starting values of the instantaneous variance rates for the HV and HW models are also fixed to the average values in Table 1. We consider a hedging horizon of one month and simulate paths over this period. We assume that there are 21 business days in a month. To be consistent with the historical analysis in the next section, we think of the simulation as starting on a Wednesday and ending on a Thursday four weeks later, spanning a total of 21 week days and 29 actual days. The security price moves according to the data-generating processes in equation (37) only on week days.

Figure 3 plots the 1,000 simulated sample paths for the security price under each of the four model environments. The pure diffusive models BS and HV generate mostly small price movements, whereas large discontinuous movements are apparent under the MJ and HW model environments.

[Figure 3 about here.]

The HV and HW models also generate stochastic volatility. We plot the corresponding simulated sample paths for the instantaneous return volatility, $\sqrt{v_t}$, in Figure 4. Given the large volatility of volatility coefficient under the HV model, several volatility sample paths hit the lower bound of zero. By incorporating jumps in the security price dynamics, the estimated stochastic volatility dynamics under HW model look more well-behaved.

[Figure 4 about here.]

At each week day, we compute the relevant option prices based on the realizations of the security price and the instantaneous variance rate, as well as the model dynamics. We monitor the hedging error (profit and loss) at each week day based on the simulated security price and the option prices. The hedging error at each date t, e_t, is defined as the difference between the value of the hedge portfolio and the value of the target call option being hedged,

$$e_t = \sum_{j=1}^{3} w_j C_t(K_j, T_j) - C_t(K, T). \tag{38}$$

Since the portfolio is derived using Taylor expansion, the initial values of the hedging portfolio and the target option may not be exactly the same. We remove this initial value mismatch through a proportional scaling of the three portfolio weights.

We hold this portfolio statically for one month and investigate the hedging error during the process and, in particular, at the end of one month. Our portfolio weights are stable over time as they depend mainly on the structural features of the option contracts such as the strike price and the relative expiration distance α. To the extent that the local volatility estimates vary over time, the standardization (d) of the strike spacing varies accordingly and so should be the portfolio weights. Nevertheless, we regard these variations as small and hold the portfolio weights fixed for the whole month while investigating its hedging performance.

We assume that option contracts are available at a finite number of strikes and maturities. That is, these

contracts can be traded at observable market prices. We exclude bid-ask spreads from our analysis. The target option choice and hedging portfolio formulation are all from this pool of available option contracts. To compute the portfolio weights, we estimate the local volatility by interpolating the implied volatility surface constructed from the finite number of option observations.

At the start of each simulation, we assume that options are available at maturities of one, two, three, six, and 12 months, and that option strikes are centered around the normalized spot price of \$100, and spaced at intervals of \$1, \$1.5, \$2, \$2.5, and \$3 for the five maturities, respectively. The assumed strike spacing increase with maturities match the behavior of SPX options market, where the strike spacing averages from \$10 to \$30 on an underlying index level of about \$1,000.

We set the target option strike at the center $K = 100$, and consider three types of maturity-strike placements for the hedge portfolio: (A) Symmetric maturity-strike triangles pointing to short maturity, with $T_c < T_o < T$, (B) symmetric maturity-strike triangles pointing to long maturity, with $T_o < T_c < T$, and (C) a line of three strikes at the same maturity ($T_h < T$). Figure 5 plots schematically the maturity-strike placement for each type. Within each type, we form ten distinct target-hedge maturity combinations out of the five available maturities. For each maturity combination, we also have many flexible choices on the strike spacing. Through this extensive simulation exercise, we strive to gain a better understanding on the dependence of the hedging performance on maturity-strike placement patterns, target-hedge maturity distances, and strike spacing.

[Figure 5 about here.]

3.3. Optimal strike spacing choice

For each maturity combination under each of the three maturity-strike placement types (A), (B), and (C), we analyze the effect of strike spacing on the hedging performance, through which we determine the optimal strike spacing choice. Given the potential instability of the portfolio weight when $d < 1$, we start at an outer strike choice close to $d = 1$ and then progressively move to the next available strike further away from K. We

perform the simulation for each strike spacing choice and record the hedging errors from 1,000 simulations. We measure the hedging performance by comparing the terminal root mean squared hedging error (RMSE) at the end of the one-month hedging exercise.

Figures 6-8 plot the terminal RMSE as a function of standardized strike spacing d under each maturity combination and each underlying dynamics for the three maturity-strike placement types (A), (B), and (C), respectively. Each figure is for one type. In each figure, each row represents one model environment, which contains ten lines grouped into three panels, with each line representing one particular maturity combination. The legend shows the combination of maturities in months in the sequence of (T_c, T_o, T) in cases (A) and (B), and (T_h, T) in case (C).

[Figure 6 about here.]

Figure 6 represents the type of the maturity-strike triangle pointing to the shorter maturity. The maturity combinations in each panel are ranked according to the relative maturity spacing measure α from high to low for the solid line, dashed line, dash-dotted line, and in the right panel, the dot-cross line. The three lines in the left panels all use one- and two-month options to form the triangle to hedge three-, six-, and 12-month options, respectively. The relative maturity spacing measure α is at one (solid line), 0.25 (dashed line), and 0.10 (dash-dotted line), respectively. Under all four models, the solid line reaches the minimum RMSE at a narrower strike spacing d than the other two lines with lower α. We label the standardized strike spacing at the lowest RMSE as the optimal strike spacing, d^*.

The three lines in the middle panels all use one-month option at the center strike and either three- or six-month options at the outer strikes to hedge six- or 12-month options. The relative maturity spacing is at $5/6$ (solid line), $2/3$ (dashed line), and $2/9$ (dash-dotted line), respectively. The four lines in the right panels use two-, three-, and six-month options to hedge six- and 12-month options, the relative maturity spacing is at $2/3$ (solid line), $1/2$ (dashed line), $1/3$ (dash-dotted line), and $1/9$ (dot-cross line). Under BS and MJ models, the optimal strike spacing shows a clear increasing pattern as α declines, but there are some exceptions to this pattern under the HV and HW models.

Figure 7 represents the case of the maturity-strike Isosceles triangle pointing to the longer maturity. The allocation of each line corresponds to that in Figure 6, except with a switch between T_c and T_o. As a result of the switch, the relative maturity spacing measures α are all negative, and the ranking from solid to dotted lines is from low (more negative) to high (less negative) α. The ranking of the optimal strike spacing across different lines also switch, with the solid lines (with more negative α) showing wider optimal strike spacing and the dotted lines (with less negative α) showing narrower optimal strike spacing. This ranking pattern stays reasonably consistent across all four models.

[Figure 7 about here.]

Figure 8 represents the degenerate case, in which all three strikes in the hedge portfolio fall on one maturity. In this case, $\alpha = 0$ for all hedge-target maturity combinations and hence it is no longer the relevant measure for comparison. The left panels contain four lines with the hedge options at one month and the target options at increasingly longer maturities from one month (solid line) to three (dashed line), six (dash-dotted line), and 12 months (dot-cross line). The optimal strike spacing decreases as the distance between the two maturities widen. The middle panels contain three lines with the hedge options all at two-month maturity and the target options at increasingly longer maturities of three (solid line), six (dashed line), and 12 months (dash-dotted line). Again, the optimal strike spacing d^* declines as the maturity distance increases. The right panel groups the remaining three lines with hedge options at three or six months and target options at six or 12 months. The distance between the target and hedge option maturity seems to play the same role as before in determining the optimal strike spacing.

[Figure 8 about here.]

Recall that the CW three-strike static strategy belongs to this degenerating case of three strikes on one maturity, except that the strike spacing in the CW strategy is pre-determined by the quadrature rule to be $d = \sqrt{3}$. However, the simulation exercises in Figure 8 show that $d = \sqrt{3}$ is rarely the optimal choice that generates the lowest root mean squared hedging error. In particular, under most simulated maturity

combinations for all four models, the optimal strike spacing is lower than the CW choice. Thus, even in this degenerating case, we can outperform the CW strategy easily via better choice of strike spacing.

Table 2 summarizes the optimal strike choice (the standardized strike spacing d^* and the dollar strike difference), the corresponding portfolio weight on the center strike (w_c), and the associated hedging performance (RMSE at the end of one month) under each of the 30 scenarios and for each of the four model environments. To quantify the observed dependence of the optimal strike spacing on the relative maturity spacing, we aggregate the results from all 30 maturity combinations under each model environment and perform the following regression analysis,

$$d^* = a + b\alpha + c(T_o/T) + e, \tag{39}$$

where α captures the relative spacing between the two hedge maturities and (T_o/T) capture the relative spacing between the target and the hedge options. The choice of the explanatory variables is largely motivated by our leading-term hedging error analysis in Section 2.3 and our observations of the simulation results in Figures 6-8. The regression results are summarized in Table 3. The regression explains about 90% of the variation under the BS model, 95% under the MJ model, but are lower at about 70% when the volatility is stochastic under HV and HW. Under all four model environments, the dependence of the optimal strike spacing on the two explanatory variables is similar. The optimal strike spacing declines with increasing relative maturity spacing between the hedge options (α), and it also declines with increasing relative maturity spacing between the hedge and the target options (T_o/T). As the ratio becomes smaller and hence the distance becomes larger, the optimal strike spacing becomes smaller. The standard errors of the coefficients also become larger in the presence of stochastic volatility. These estimated relations can guide our strike space in practical applications.

3.4. Hedging performance comparisons

To understand how the hedging performance varies across different maturity-strike scenarios, Figure 9 plots the root mean squared hedging error as a function of a maturity distance measure (T/T_h) between the target

and the hedge options. For hedge portfolios spanning two maturities, T_h represents the weighted average maturity of the hedge portfolio. The plots show that as the target option becomes further away from the hedge options, the hedging error increases. The solid line represents a nonparametric fitting of the increasing relation, which highlights the virtue of hedging with "nearby" contracts. The increasing relations are quite clear under the BS and MJ environment, but become much noisier in the presence of stochastic volatility under the HV and HW model environments. The hedging errors are also larger in the presence of stochastic volatility.

[Figure 9 about here.]

To gauge the relative effectiveness of our proposed hedging strategies, we also compare their performance to the performance of delta hedging using the underlying futures with daily rebalancing frequency. Delta hedging with daily frequency represents the common practice of the industry. Following each simulated sample path, we compute the Black-Scholes delta of the option at its current implied volatility level at each date and rebalance the futures position accordingly. In principle, one can compute the delta based on the underlying security price dynamics. Yet, since investors do not know the exact dynamics for the underlying, we follow the common industry practice by using the Black-Scholes formula to compute the delta at the observed implied volatility level of the option. The hedging error at each date t can be computed as,

$$e_t = B_{t-1}e^{rh} + \Delta_{t-1}(F_t - F_{t-1}) - C(S_t, t; K, T), \tag{40}$$

where Δ_t denotes the delta of the target call option with respect to the futures price at time t, h denotes the daily time interval between stock trades, and B_t denotes the time-t balance in the money market account. The balance includes the receipts from selling the target call option, less the cost of initiating and possibly changing the hedge portfolio.

Table 4 reports the root mean squared hedging error after one month of daily delta hedging on four different target options under the four different model environments. The delta hedging works remarkably

well under the Black-Scholes environment, with RMSE ranging from 0.08 to 0.21, but the hedging error increases by several folds once we include jumps and stochastic volatilities in the dynamics. For all models, the hedging error tends to be larger on shorter-term contracts given the higher gamma on these options.

Comparing the delta hedging performance in Table 4 with that from our static three-strike portfolios in Figure 9, we observe that under the BS model, to outperform delta hedging on the two-month option (with RMSE of 0.21), we need a maturity ratio T/T_h less than six times for our three-strike strategy. For example, a line of three strikes at one month will perform dramatically better by generating an RMSE of 0.04. To beat the delta hedging performance on the three-month option with RMSE at 0.17, any strategies with T/T_h less than five will surface. For example, the maturity-strike triangle with center strike at one-month and outer strikes at two-month maturity generates an RMSE of merely 0.02. Beating the delta-hedging performance on the 6-month option at RMSE of 0.12 and the performance on 12-month option at RMSE of 0.08 become harder as we need further reduce the target-hedge maturity distance T/T_h to be within three or two. For example, using a two-month option at the center strike and two three-month options at the outer strike to hedge the six-month option generates an RMSE of 0.05; using a three-month option at center strike and two six-month options at the two outer strikes to hedge the 12-month option also generates an RMSE of 0.05. These examples show that under the BS model environment, our static strategy with three options can outperform the delta-hedging if we choose the hedge option maturities not too far away from the target option maturity.

When we allow jumps in the security price dynamics under the MJ model, the delta-hedging performance deteriorates dramatically. The RMSE is between 0.43 to 0.86. In this case, any of the 30 simulated maturity-strike combinations can outperform the delta-hedging strategy, even when the target option maturity is 12 times as large as the hedge option maturity. The maximum RMSE from the 30 combinations is 0.25, when we hedge the 12-month option with three one-month options.

In the presence of stochastic volatility under HV, the delta hedging performance also deteriorates dramatically. The RMSE is between 0.68 to 0.95. By contrast, the worst performing combination out of our 30 simulated case has an RMSE of 0.59 from the line of three strikes at one-month maturity to hedge the

six-month option.

The delta-hedging performance further deteriorates when we incorporate both stochastic volatility and discontinuous price movements in HW, the RMSE is between 0.86 and 1.08. By contrast, the largest root mean squared hedging error from our three-strike static hedge combinations is 0.54, again from the line of three strikes at one-month maturity to hedge the six-month option.

To visualize the performance difference under different model environments, Figure 10 plots the the simulated sample paths of the hedging errors on the 12-month option hedged with (i) daily delta hedging with the underlying futures and (ii) the maturity-strike triangle with the center strike at two-month maturity and the outer strikes at one-month maturity. The delta hedging of the 12-month option generates the best delta-hedging performance among the four candidate target options. On the other hand, the chosen triangle is the farthest away from the target option in terms of maturity distance. Thus, we are comparing the best scenario from the delta hedging with the worst scenario from a maturity-strike triangle.

[Figure 10 about here.]

Under the BS model environment, the delta hedging generates smaller average hedging errors with an RMSE of 0.08 whereas the RMSE from the triangle is 0.21. Delta-hedging of a short option position remains short in gamma and as such, the hedging error distribution is negatively skewed: One loses money whenever there is big movements. By contrast, the triangle generates positive skewness in the hedging error distribution. By long the triangle, the hedged portfolio has turned positive in gamma instead.

Under the MJ model environment, whenever the underlying security price experiences a large jump of either direction, the delta-hedged portfolio experience a large negative error. The hedging error is strongly negatively skewed, and the hedging loss can be as high as \$6. By contrast, the original receipt from the sale of the 12-month target option is only 9.18.[3] On the other hand, the triangle hedges both the small and large moves well and generate a reasonably symmetric hedging error distribution, as the hedging errors are constrained on either side. The maximum loss is less than \$0.4 whereas the maximum gain is less than \$0.7.

[3]The initial value of the 12-month target option is 9.55 under the BS model, 8.38 under the HV model, and 8.30 under the HW model.

The terminal RMSE is 0.43 from delta hedging versus 0.16 from the triangle.

Under the HV model environment, the terminal RMSE is 0.68 from delta hedging versus 0.26 from the triangle. In particular, the hedging error from the triangle hedge grows more slowly than that from the delta hedge, especially at the first two weeks.

Under the HW model environment that includes both jumps and stochastic volatility, it is the jumps that generate the largest hedging errors for delta hedging. By contrast, the triangle hedge remains stable in this environment. The terminal RMSE is 0.86 for delta hedging versus 0.41 for the triangle.

Figure 11 compares the cumulation of the RMSE over time for the two strategies, with the solid line for the maturity-strike triangle and the dashed line for the delta hedging. To ease the comparison, we use the same scale for all four panels. The comparison reveals two major points. First, the triangle generates higher RMSE's than the delta-hedging under the BS environment, but performs better in all other model environments. Second, the delta hedging generates very small RMSE under the BS model, but the error increases drastically in the presence of jump and/or stochastic volatility. The terminal RMSE increases by over 10 times from 0.08 to 0.86 as the model environment switches from BS to HW. By contrast, the triangle hedge performance is much less sensitive to variations in the model environment. The terminal RMSE stays within a narrow range from 0.16 to 0.41 as the environment changes.

[Figure 11 about here.]

These simulation exercises show that our proposed three-strike static hedge dominates the daily rebalancing delta hedging in terms of the root mean squared hedging errors. Furthermore, although our hedge portfolios are derived using Taylor expansions of nearby option contracts, due to the expansion error cancelation between the target option and the hedge portfolio, the strategy works well even when target option is far away from the hedge portfolio. In particular, even when the target option maturity is over ten times longer than the average maturity of the hedge portfolio, the hedging performance remains better than the performance from the delta hedging benchmark, especially when the underlying dynamics include the commonly observed features such as discontinuous price movements and stochastic volatility.

Finally, since our strategy allows extremely flexible choices in both strikes and maturities, market makers can use our proposal to judge and act on incoming order flows by balancing the transaction benefit with hedging efficiency. Risk managers can also judiciously choose option contracts to balance the risk of the option portfolio while minimizing transaction cost.

4. A Historical Hedging Exercise on S&P 500 Index Options

In this section, we investigate the historical performance of our strategies in hedging the sale of S&P 500 index options. We obtain data on S&P 500 index (SPX) options from January 1996 to March 2009. These options are standard European options on the spot index and are listed at the Chicago Board of Options Exchange (CBOE). The data set includes, among other information, the closing quotes on each options contract. Our hedging exercises are based on the mid option price quotes.

Our historical analysis on SPX options is in parallel with the simulation exercise in the previous section. Over our sample period, we identify 158 starting dates from January 17, 1996 to February 18, 2009, when there are options expiring exactly 30 days after. Since the S&P 500 index options expire on the Saturday following the third Friday and the terminal payoff is computed based on the opening price on that Friday morning, trades and quotes on the expiring options effectively stop on the preceding Thursday, and our chosen starting dates in each month all fall on a Wednesday. At each starting date, we form hedging portfolios and hold the portfolios statically for 30 days. We compute summary statistics on the hedging errors based on the 158 repeated exercises. The hedging errors from all exercises are normalized to be in percentages of the index level at the start of the exercise.

From each starting date, options are always available at one-month maturity (31 days) by design. Two-month options are also available for all starting dates, but the maturity availability after the two-month maturity varies across starting dates. For our hedging exercise, we classify options into four maturity groups: (i) one-month options (31 days), (ii) two-month options (59 or 66 days), (iii) options with maturities three to five months (87-157 days), and (iv) options with maturities around one year (276-402 days). For convenience, we refer to the latter two groups as four-month and 12-month options, respectively. Based on the

four maturities groups, we can form 14 target-hedge portfolio maturity combinations, with four satisfying $T_o < T_c < T$, four satisfying $T_c < T_o < T$, and the remaining six satisfying $T_c = T_o < T$.

In each of the 14 combinations, we choose the target option strike close to the spot level. To choose the strike spacing for the hedging portfolio, we use the regression results in Table 3 under the HW model to estimate the optimal strike spacing d^* as a function of α and T_o/T. Choosing d^* based on the simulation results from the other three models generates similar results. Given d^*, we compute ΔK and the portfolio weight based on the local volatility estimate $\sigma(K, T_o)$ and the maturity placement α. Then, we choose the three available strikes for the hedging portfolio that are closest to the projected optimal strike spacing.

Figure 12 plots the terminal root mean squared hedging error from the 14 different maturity-strike combinations. The hedging errors are larger than the four simulated cases in Figure 9 due to constraints on strike availability and the possibility that the SPX index dynamics are more complicated than those simulated. For comparison, we also perform the delta hedging with the underlying futures with daily rebalancing. The root mean squared hedging errors on two-, four-, and 12-month options are 0.63, 0.63, and 0.66, respectively. Of the 14 maturity combinations for our static strategy, only three generate root mean squared errors larger than 0.63. In particular, our static strategy performs better as long as the target option maturity is less than five times the average hedge option maturity.

[Figure 12 about here.]

We follow both strategies for 29 actual days, running from the starting date to the Thursday of the fourth following week, the last day of trading for the one-month options used in the static hedge. Figure 13 plots the sample paths of the hedging errors from selected strategies. The three panels on the left side are from maturity-strike triangles hedging from top to bottom two-, four-, and 12-month options. The three panels on the right side are from daily delta hedging of the same target option. The hedging errors from the triangles are visibly smaller over the whole sample paths than that from the daily delta hedge.

[Figure 13 about here.]

5. Concluding Remarks

Most existing hedging methodologies are based on neutralizing risk exposures defined under a pre-specified model. In this paper, we propose a new hedging approach based on the affinity of the derivative contracts. As a result, the formulation of the hedging strategy does not depend on the assumptions on the underlying risk dynamics, but only depend on the strike and maturity of the option contracts available for forming the hedge portfolio. In hedging a target option, we focus on hedge portfolios of three options at three different strikes and two different maturities that form a stable maturity-strike triangle, and we derive the portfolio weights for the hedge portfolio as a function of the strike and maturity spacing of the triangle relative to the target option. Numerical analysis under commonly proposed security price dynamics shows that the hedging performance of our methodology based on static positions of three options compares favorably against the dynamic delta hedging strategy with daily rebalancing. In particular, when many strikes are available for forming the hedging portfolio, we can choose the strike spacing judiciously to further optimize the hedging performance, making the strategy work well even when the maturities of the target and hedge options are far apart. A historical hedging exercise on S&P 500 index option further highlights the superior performance of our strategies.

References

Bakshi, G., C. Cao, and Z. Chen, 1997, "Empirical Performance of Alternative Option Pricing Models," *Journal of Finance*, 52(5), 2003–2049.

Bakshi, G., and N. Kapadia, 2003, "Delta-Hedged Gains and the Negative Market Volatility Risk Premium," *Review of Financial Studies*, 16(2), 527–566.

Bates, D. S., 1996, "Jumps and Stochastic Volatility: Exchange Rate Processes Implicit in Deutsche Mark Options," *Review of Financial Studies*, 9(1), 69–107.

Bates, D. S., 2003, "Empirical Option Pricing: A Retrospection," *Journal of Econometrics*, 116(1), 387–404.

Bhattacharya, M., 1980, "Empirical Properties of the Black-Scholes Formula under Ideal Conditions," *Journal of Financial and Quantitative Analysis*, 15(5), 1081–1105.

Black, F., and M. Scholes, 1973, "The Pricing of Options and Corporate Liabilities," *Journal of Political Economy*, 81(3), 637–654.

Boyle, P. P., and D. Emanuel, 1980, "Discretely Adjusted Option hedges," *Journal of Financial Economics*, 8, 259–282.

Breeden, D. T., and R. H. Litzenberger, 1978, "Prices of State-Contingent Claims Implicit in Option Prices," *Journal of Business*, 51(4), 621–651.

Carr, P., and A. Chou, 1997, "Breaking Barriers," *Risk*, 10(9), 139–145.

Carr, P., and D. Madan, 1998, "Towards a Theory of Volatility Trading," in *Risk Book on Volatility*, ed. by R. Jarrow. Risk, New York, pp. 417–427.

Carr, P., and L. Wu, 2002, "Static Hedging of Standard Options," working paper, New York University and Baruch College.

Carr, P., and L. Wu, 2003, "Finite Moment Log Stable Process and Option Pricing," *Journal of Finance*, 58(2), 753–777.

Coleman, T. F., Y. Li, and A. Verma, 1998, "Reconstructing The Unknown Local Volatility Function," *Journal of Computational Finance*, 2(3), 77–102.

Dumas, B., J. Fleming, and R. E. Whaley, 1998, "Implied Volatility Functions: Empirical Tests," *Journal of Finance*, 53(6), 2059–2106.

Dupire, B., 1994, "Pricing with a Smile," *Risk*, 7(1), 18–20.

Figlewski, S., 1989, "Options Arbitrage in Imperfect Markets," *Journal of Finance*, 44(5), 1289–1311.

Galai, D., 1983, "The Components of the Return from Hedging Options Against Stocks," *Journal of Business*, 56(1), 45–54.

Gatheral, J., 2006, *The Volatility Surface: A Practitioner's Guide*. John Wiley & Sons, New Jersey.

Green, R., and R. A. Jarrow, 1987, "Spanning and Completeness in markets with Contingent Claims," *Journal of Economic Theory*, 41, 202–210.

Heston, S. L., 1993, "Closed-Form Solution for Options with Stochastic Volatility, with Application to Bond and Currency Options," *Review of Financial Studies*, 6(2), 327–343.

Huang, J., and L. Wu, 2004, "Specification Analysis of Option Pricing Models Based on Time-Changed Lévy Processes," *Journal of Finance*, 59(3), 1405–1440.

Kennedy, J., P. Forsyth, and K. Vetzal, 2006, "Calibration and Hedging under Jump Diffusion," *Review of Derivatives Research*, 9(1), 1–35.

Kennedy, J., P. Forsyth, and K. Vetzal, 2009, "Dynamic Hedging under Jump Diffusion with Transaction Cost," *Operations Research*, 57(3), 541–559.

Lee, R. W., 2005, "Implied Volatility: Statics, Dynamics, and Probabilistic Interpretation," in *Recent Advances in Applied Probability*, ed. by R. Baeza-Yates, J. Glaz, H. Gzyl, J. Hüsler, and J.L.Palacios. Springer, New York, pp. 241–268.

Leland, H. E., 1985, "Option Pricing and Relation with Transaction Costs," *Journal of Finance*, 40(5), 1283–1301.

Merton, R. C., 1973, "An Intertemporal Asset Pricing Model," *Econometrica*, 41, 867–887.

Merton, R. C., 1976, "Option Pricing When Underlying Stock Returns Are Discontinuous," *Journal of Financial Economics*, 3(1), 125–144.

Nachman, D., 1988, "Spanning and Completeness with Options," *Review of Financial Studies*, 3(31), 311–328.

Ross, S. A., 1976, "Options and Efficiency," *Quarterly Journal of Economics*, 90, 75–89.

Takahashi, A., and A. Yamazaki, 2009a, "Efficient Static Replication of European Options under Exponential Lvy Models," *Journal of Futures Markets*, 29(1), 1–15.

Takahashi, A., and A. Yamazaki, 2009b, "A New Scheme for Static Hedging of European Derivatives under Stochastic Volatility Models," *Journal of Futures Markets*, 29(5), 397–413.

Toft, K. B., 1996, "On the Mean-Variance Tradeoff in Option Replication with Transactions Costs," *Journal of Financial and Quantitative Analysis*, 31(2).

Table 1
Model parameters used in the simulation analysis

Model	$\sqrt{\theta}$	λ_0	μ_j	σ_j	$\sqrt{v_t}$	κ	ω	ρ
BS	0.2277	—	—	—	—	—	—	—
MJ	0.1869	14.30	-0.1021	0.1432	—	—	—	—
HV	0.2277	—	—	—	0.1864	3.7863	0.9095	-0.6824
HW	0.1869	14.30	-0.1021	0.1432	0.1650	1.8766	0.3811	-0.7564

Table 2

Hedging performance at different maturity-strike placements and model environments

Entries report the root mean squared hedging error (RMSE) after one month under different scenarios, with the strike spacing chosen to minimize the RMSE. The table also reports the strike spacing (d^* and ΔK) for each corresponding hedging portfolio.

Maturity\Model			BS				MJ				HV				HW			
T_c	T_o	T	d^*	ΔK	w_c	RMSE	d^*	ΔK	w_c	RMSE	d^*	ΔK	w_c	RMSE	d^*	ΔK	w_c	RMSE
1	2	3	1.14	7.5	0.13	0.02	1.16	7.0	0.15	0.05	0.67	3.5	-0.38	0.22	0.66	3.5	-0.40	0.18
1	2	6	1.29	17.0	0.35	0.13	1.29	15.5	0.35	0.14	1.29	13.5	0.35	0.52	1.17	12.5	0.23	0.49
1	2	12	1.27	26.5	0.36	0.29	1.24	23.5	0.32	0.23	1.24	20.5	0.33	0.45	1.19	20.0	0.27	0.50
1	3	6	1.14	13.0	0.15	0.06	1.18	12.5	0.19	0.10	1.08	10.0	0.09	0.40	0.95	9.0	-0.06	0.37
1	3	12	1.27	25.0	0.33	0.23	1.26	23.0	0.32	0.22	1.25	20.0	0.31	0.41	1.19	19.5	0.25	0.48
1	6	12	1.09	17.5	0.09	0.07	1.15	17.5	0.15	0.11	1.25	17.5	0.24	0.33	1.10	15.5	0.10	0.36
2	3	6	1.36	15.5	0.39	0.05	1.42	15.0	0.43	0.07	1.84	17.0	0.64	0.25	0.69	6.5	-0.66	0.37
2	3	12	1.42	28.0	0.48	0.17	1.36	25.0	0.44	0.15	1.44	23.0	0.49	0.23	1.37	22.5	0.44	0.39
2	6	12	1.21	19.5	0.22	0.06	1.21	18.5	0.22	0.09	1.61	22.5	0.49	0.21	1.35	19.0	0.33	0.33
3	6	12	1.27	20.5	0.29	0.05	1.35	20.5	0.35	0.08	1.76	24.5	0.58	0.15	1.64	23.0	0.53	0.26
2	1	3	1.77	16.5	0.81	0.04	1.72	14.5	0.80	0.04	2.25	16.5	0.89	0.18	1.83	13.5	0.82	0.18
2	1	6	1.56	23.0	0.64	0.12	1.47	19.5	0.59	0.10	1.72	20.0	0.71	0.30	1.50	17.5	0.61	0.39
2	1	12	1.47	32.0	0.56	0.21	1.34	26.5	0.47	0.16	1.42	24.5	0.53	0.26	1.33	23.0	0.46	0.41
3	1	6	1.70	25.0	0.76	0.08	1.58	21.0	0.71	0.06	1.81	21.0	0.79	0.16	1.71	20.0	0.76	0.25
3	1	12	1.56	34.0	0.64	0.16	1.44	28.5	0.57	0.12	1.48	25.5	0.59	0.16	1.44	25.0	0.57	0.31
6	1	12	1.79	39.0	0.80	0.07	1.60	31.5	0.74	0.06	1.54	26.5	0.71	0.06	1.62	28.0	0.75	0.13
3	2	6	1.71	22.5	0.72	0.06	1.62	19.5	0.68	0.06	1.87	19.5	0.77	0.15	1.78	19.0	0.74	0.25
3	2	12	1.59	33.0	0.63	0.14	1.42	27.0	0.53	0.12	1.46	24.0	0.55	0.15	1.45	24.5	0.55	0.31
6	2	12	1.78	37.0	0.78	0.07	1.63	31.0	0.73	0.06	1.58	26.0	0.71	0.05	1.69	28.5	0.76	0.13
6	3	12	1.80	35.5	0.77	0.06	1.64	30.0	0.72	0.06	1.62	26.0	0.71	0.05	1.74	28.5	0.75	0.12
1	1	2	1.52	10.0	0.57	0.04	1.51	9.0	0.56	0.07	1.83	9.5	0.70	0.42	1.53	8.0	0.57	0.26
1	1	3	1.45	13.5	0.53	0.10	1.43	12.0	0.51	0.11	1.63	12.0	0.63	0.55	1.35	10.0	0.45	0.40
1	1	6	1.36	20.0	0.46	0.21	1.32	17.5	0.42	0.18	1.42	16.5	0.50	0.59	1.24	14.5	0.35	0.54
1	1	12	1.33	29.0	0.43	0.32	1.24	24.5	0.35	0.25	1.28	22.0	0.39	0.47	1.15	20.0	0.25	0.53
2	2	3	1.52	10.0	0.57	0.01	1.66	10.0	0.64	0.03	2.69	14.0	0.86	0.17	2.06	11.0	0.76	0.17
2	2	6	1.52	20.0	0.57	0.09	1.45	17.5	0.53	0.09	1.73	18.0	0.66	0.29	1.55	16.5	0.58	0.37
2	2	12	1.44	30.0	0.52	0.19	1.37	26.0	0.46	0.15	1.46	24.0	0.53	0.25	1.33	22.5	0.44	0.40
3	3	6	1.58	18.0	0.60	0.04	1.61	17.0	0.61	0.05	2.00	18.5	0.75	0.13	1.90	18.0	0.72	0.23
3	3	12	1.55	30.5	0.58	0.13	1.47	27.0	0.54	0.12	1.53	24.5	0.57	0.14	1.52	25.0	0.57	0.30
6	6	12	1.65	26.5	0.63	0.04	1.64	25.0	0.63	0.05	1.90	26.5	0.72	0.09	1.99	28.0	0.75	0.11

Table 3

Relating optimal strike spacing to relative maturity spacing among hedge and target options

Entries in panel A report results from the following regression

$$d^* = a + b\alpha + c(T_o/T) + e,$$

where the optimal strike spacing (d^*) is related to the relative maturity spacing between the hedge options α and the relative maturity spacing between the hedge and target options (T_o/T) under each model environment. In parentheses are standard errors of the parameter estimates. The last column reports the R-squares of the regressions.

Model	a		b		c		R^2
BS	1.3843	(0.0292)	-0.6210	(0.0423)	0.3899	(0.0890)	0.8981
MJ	1.2383	(0.0168)	-0.5661	(0.0244)	0.6976	(0.0513)	0.9491
HV	1.0495	(0.0837)	-1.0712	(0.1212)	1.9006	(0.2549)	0.7430
HW	1.1082	(0.0886)	-0.9661	(0.1283)	1.2072	(0.2697)	0.6623

Table 4

Performance of delta hedging with daily rebalance

Entries report the root mean squared hedging error after one month from delta hedging with the underlying futures on four different target options with daily rebalancing under different model environments.

T	BS	MJ	HV	HW
2	0.21	0.85	0.88	1.08
3	0.17	0.76	0.95	1.07
6	0.12	0.60	0.89	1.02
12	0.08	0.43	0.68	0.86

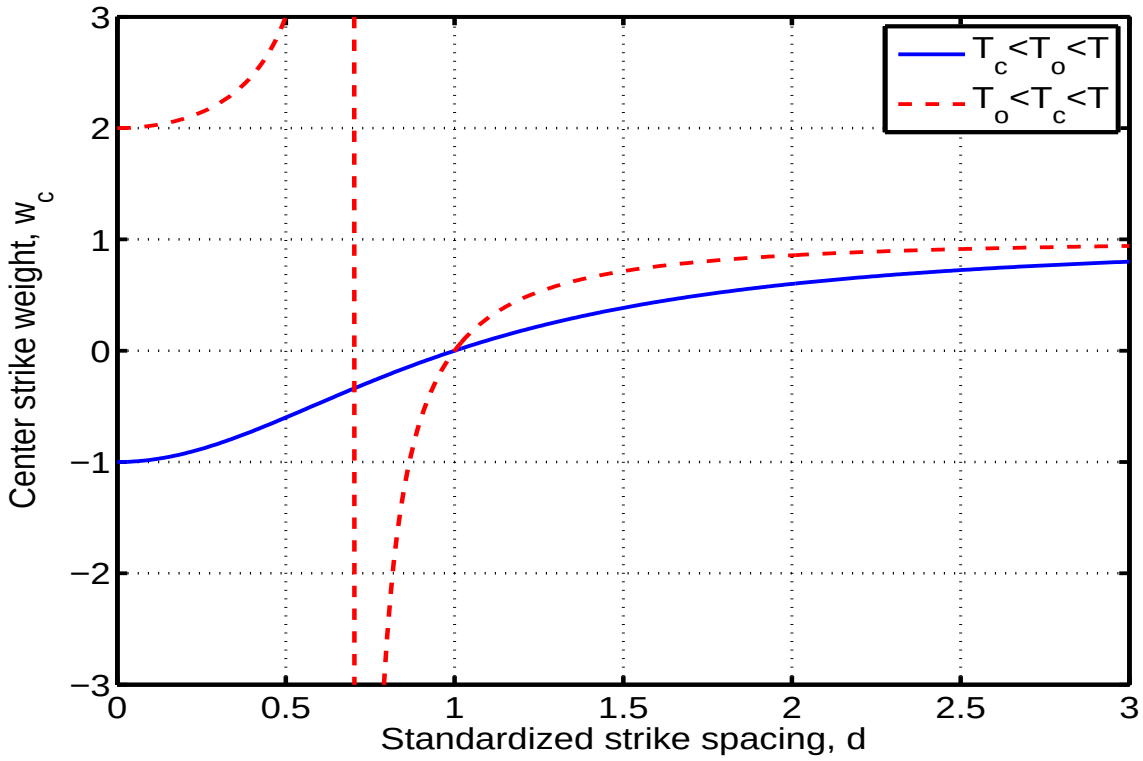

Figure 1. Portfolio weight in the maturity-strike triangle as a function of strike spacing.
Lines show the portfolio weight on the center strike (w_c) in the symmetric maturity-strike triangle as a function of the standardized strike spacing measure d for two maturity rankings: (i) $T_c < T_o < T$ (solid line) and (ii) $T_o < T_c < T$ (dashed line). The plots are generated with equal spacing between the three maturities: $\alpha = 1$ for the solid line and $\alpha = -1/2$ for the dashed line.

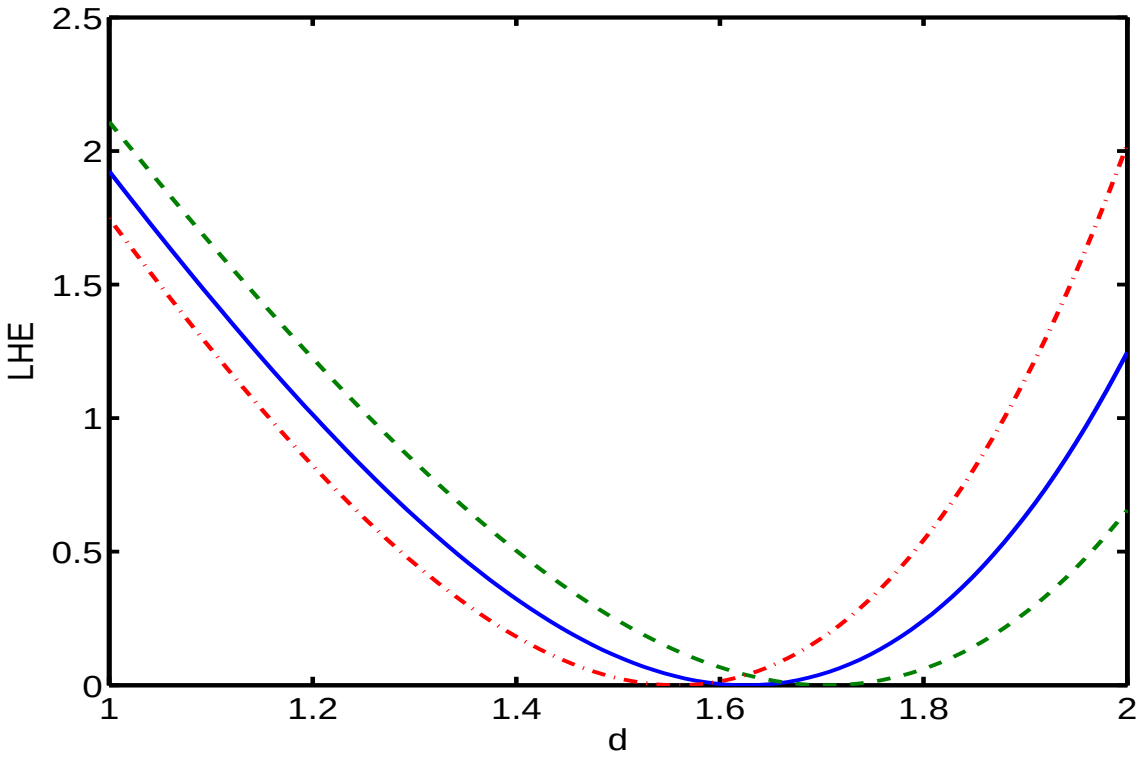

Figure 2. Expansion error as a function of strike spacing for several target strikes.
Each curve represents the leading-term hedging error as a function of d, where we assume a Black-Scholes model with $\sigma = 0.25$, zero rates, and the maturities (T_c, T_o, T) at one, two, and six months, respectively. The three lines represent target option strikes at $K =$ \$90 (dashed line), \$100 (solid line), and \$110 (dash-dotted line), respectively, relative to a normalized spot level of \$100.

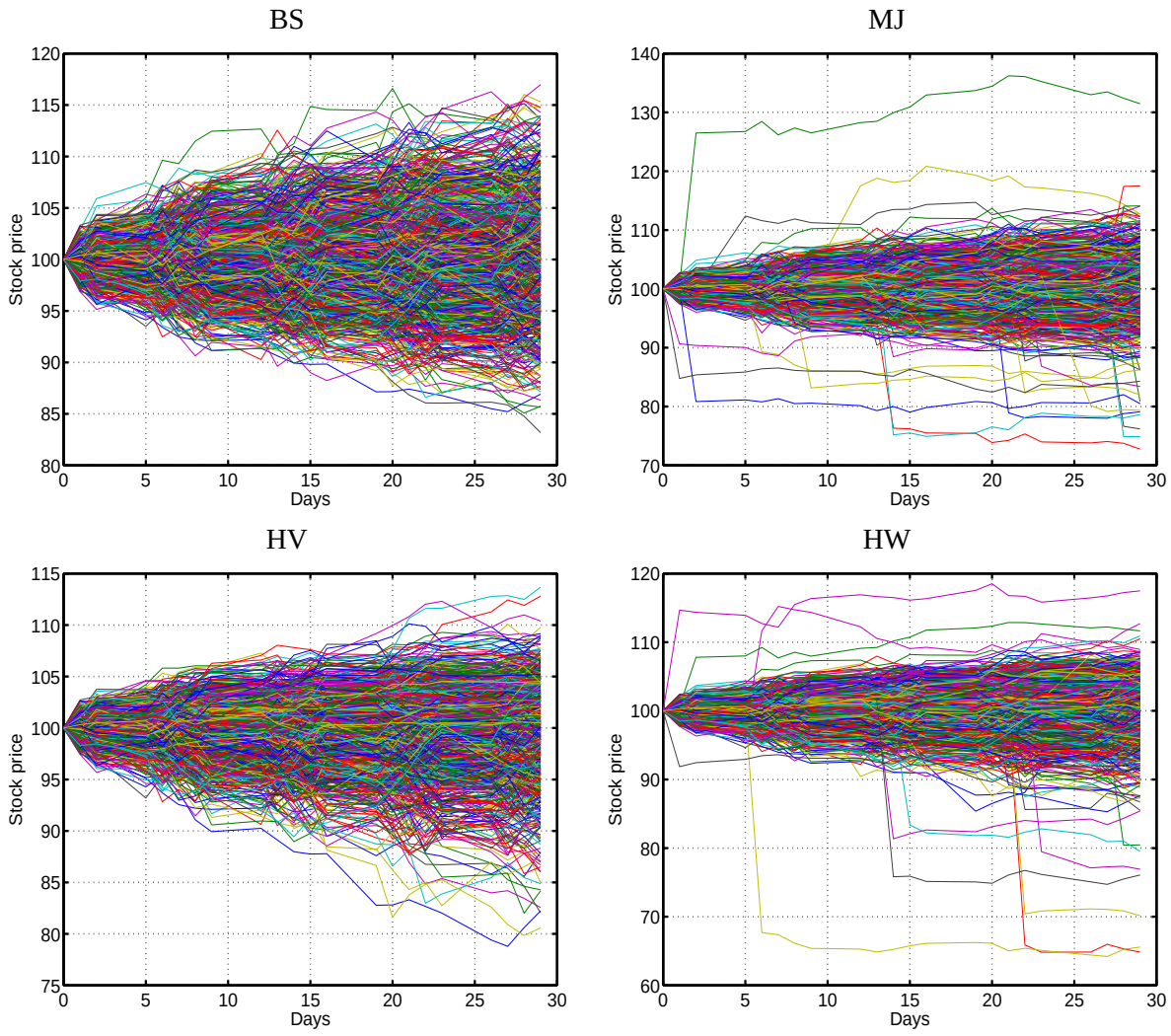

Figure 3. Simulated sample paths for the security price under different models.
Lines represent the simulated sample paths for the security price under different model environments.

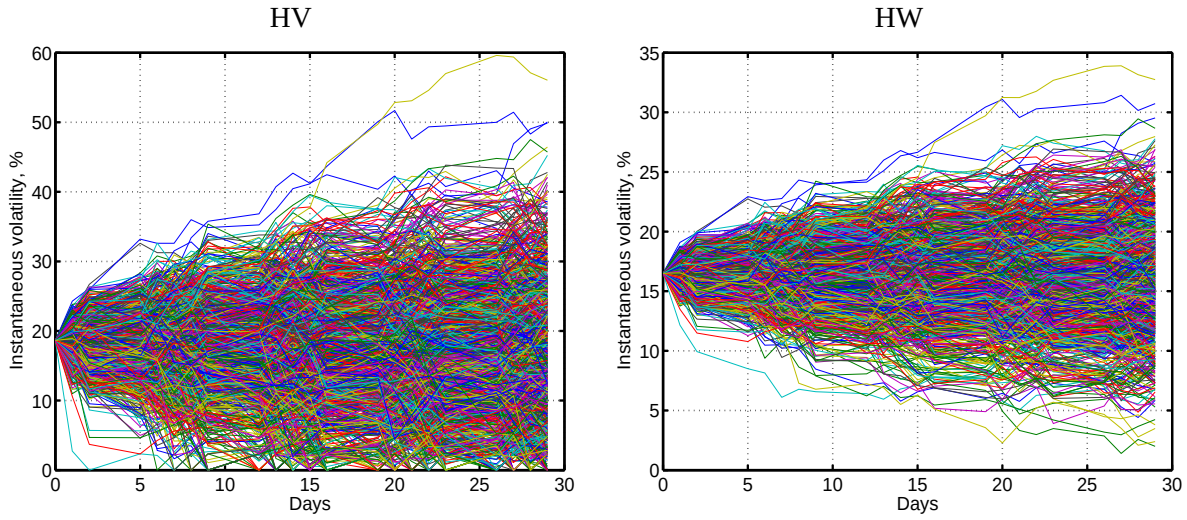

Figure 4. Simulated sample paths for the instantaneous volatility under stochastic volatility models. Lines represent the simulated sample paths for the instantaneous volatility, $\sqrt{v_t}$, under the HV (left panel) and HW (right panel) model, respectively.

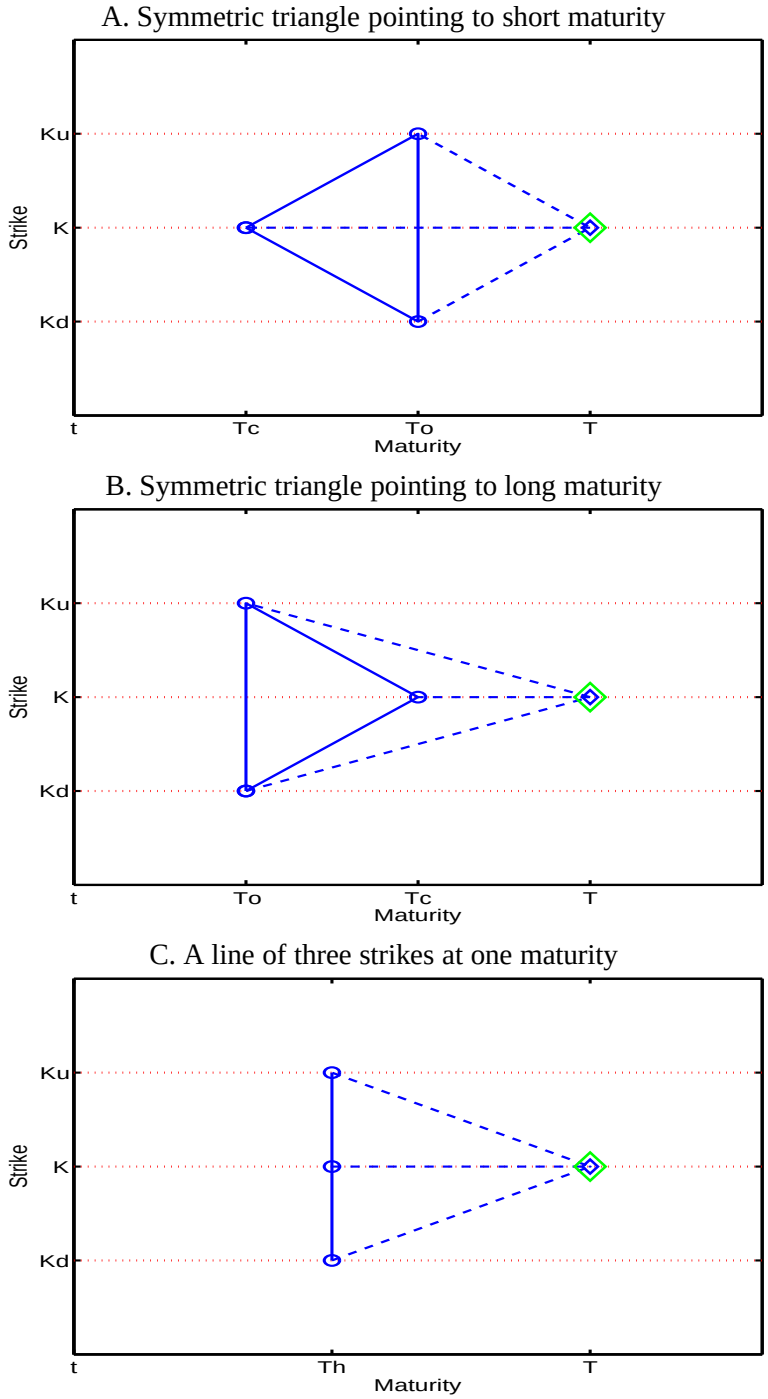

Figure 5. Schematic placements of three options to hedge a target option.
The target option at strike K and maturity T is denoted as a double-layer diamond. The three hedging options at strikes $K_d < K < K_u$ are denoted in circles are lined by a solid line, where the center strike maturity is denoted T_c and the outer strike maturity is denoted as T_o. When all three options in the hedge portfolio are at one maturity, it is denoted as T_h.

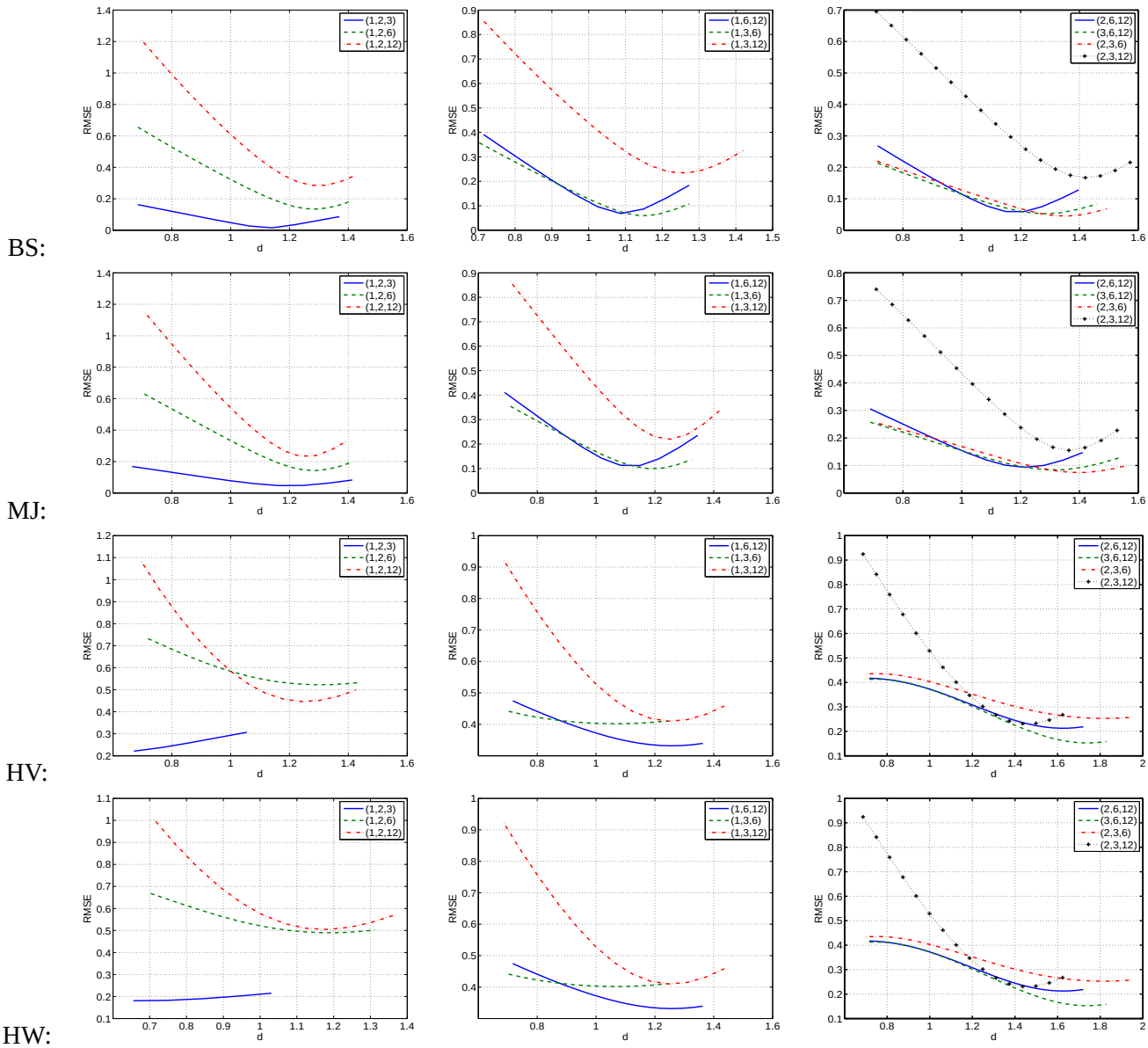

Figure 6. Effects of maturity and strike spacing on hedging performance when $T_c < T_o < T$.
Each row represents one model, which contains ten lines grouped into three panels, with each line representing one particular maturity combination (T_c, T_o, T) shown in the legend. The maturity combinations in each panel are ranked according to the relative maturity spacing measure α from high to low for the solid line, dashed line, dash-dotted line, and in the right panels, the dot-cross line.

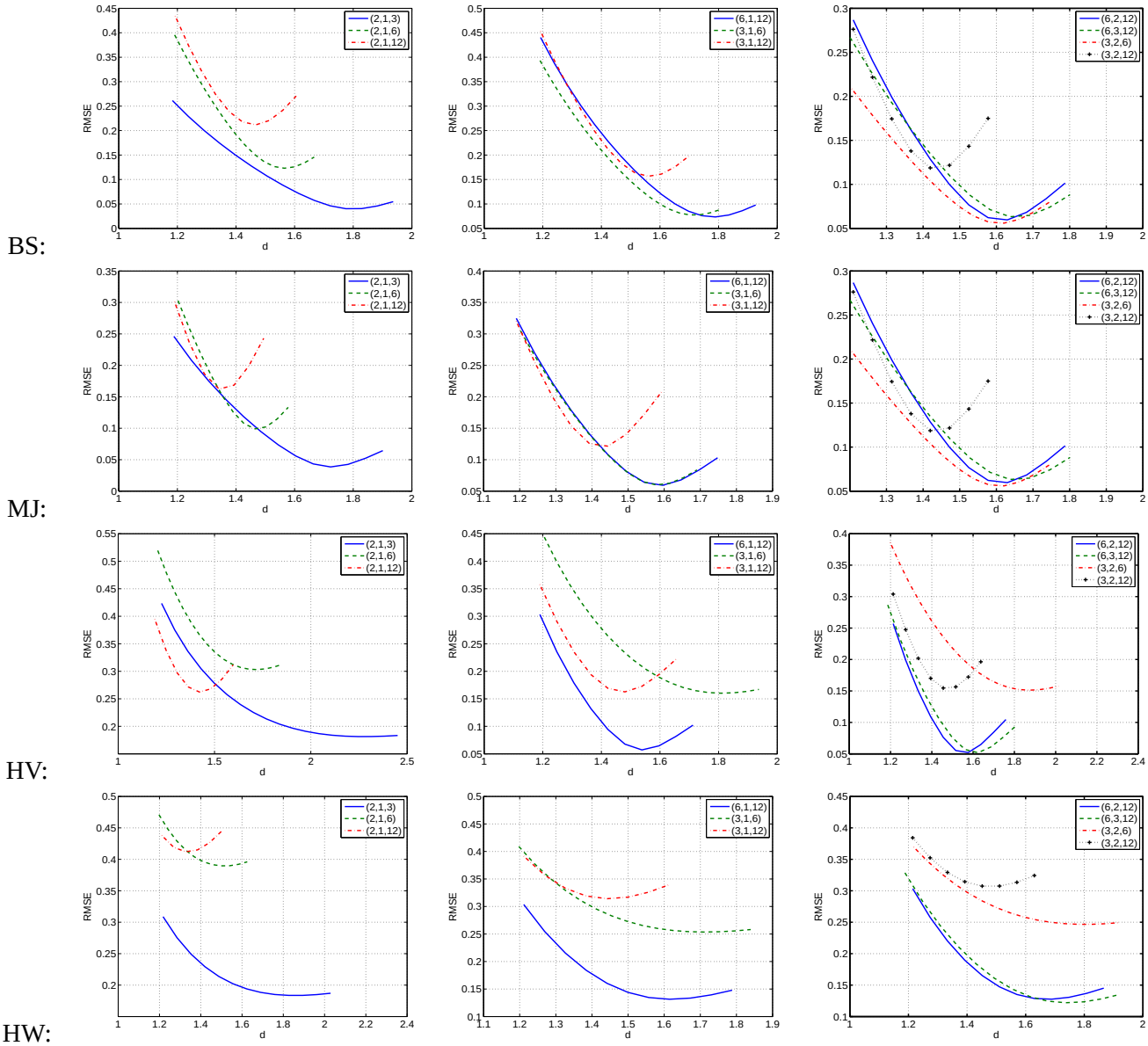

Figure 7. Effects of maturity and strike spacing on hedging performance when $T_o < T_c < T$.
Each row represents one model, which contains ten lines grouped into three panels, with each line representing one particular maturity combination (T_c, T_o, T) shown in the legend. The maturity combinations in each panel are ranked according to the relative maturity spacing measure α from high to low for the solid line, dashed line, dash-dotted line, and in the right panels, the dot-cross line.

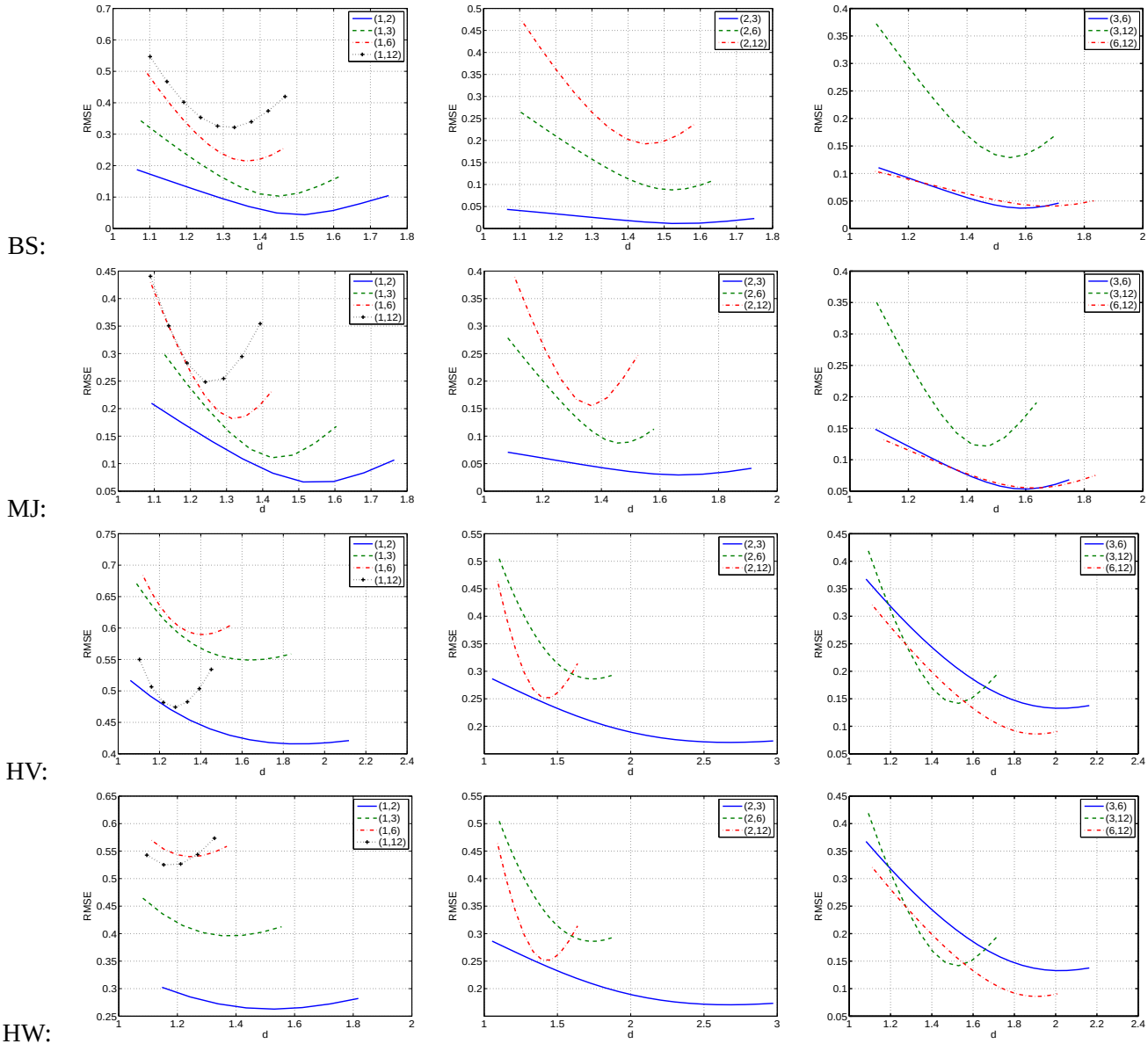

Figure 8. Effects of maturity and strike spacing on hedging performance when $T_c = T_o < T$.
Each row represents one model, which contains ten lines grouped into three panels, with each line representing one particular maturity combination of hedge-target options (T_h, T) shown in the legend.

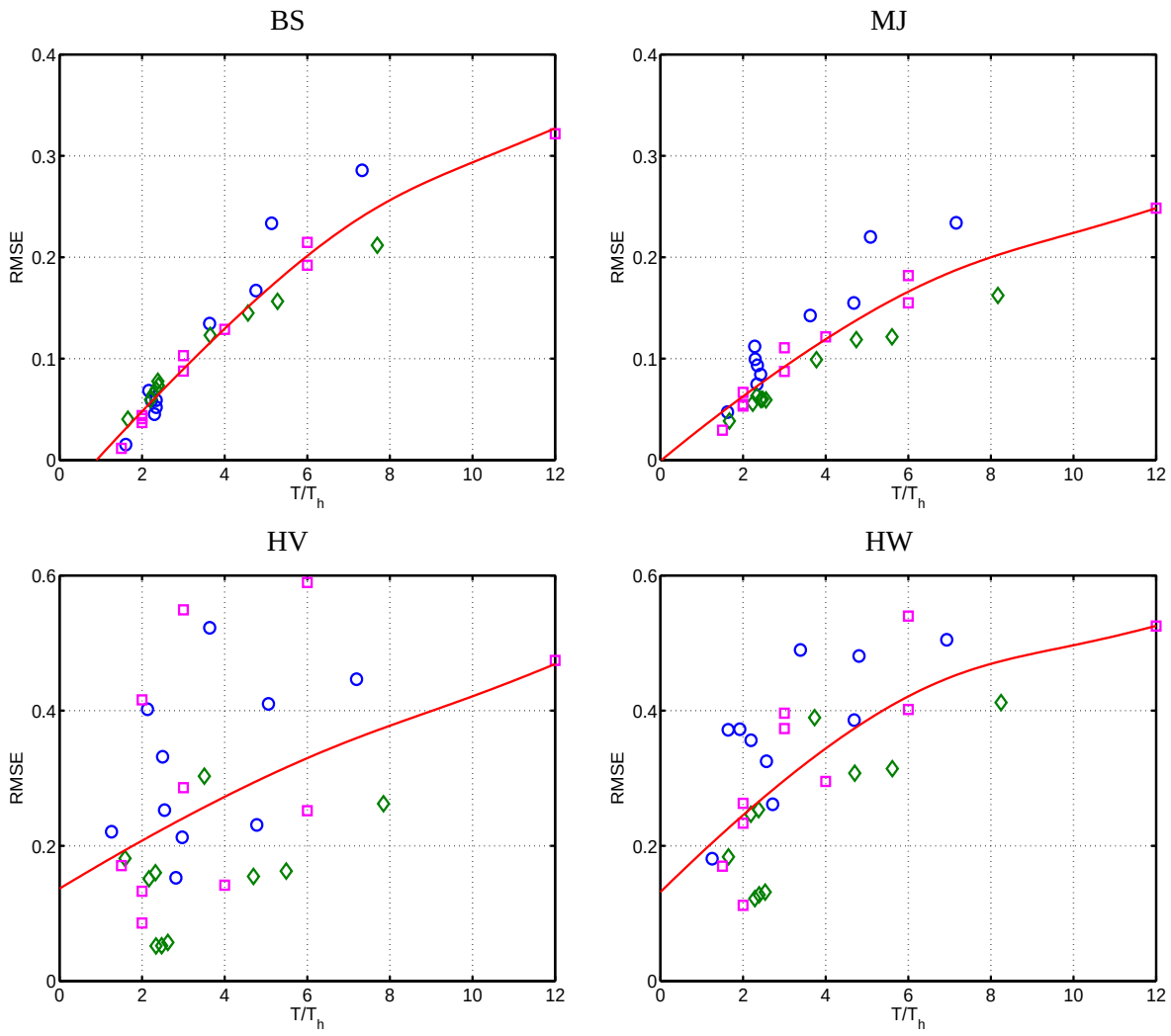

Figure 9. Dependence of hedging performance on target/hedge maturity difference T/T_h.
We measure the maturity distance as the ratio of the target option maturity to the average maturity of options in the hedge portfolio (T/T_h), and we plot the root mean squared hedging error at optimal strike spacing as a function of this maturity ratio. The circles represent maturity-strike triangles with $T_c < T_o < T$; the diamonds represent maturity-strike triangles with $T_o < T_c < T$; and the squares represent the hedge portfolios of three strikes at one maturity $T_h < T$. Each panel is for one underlying model.

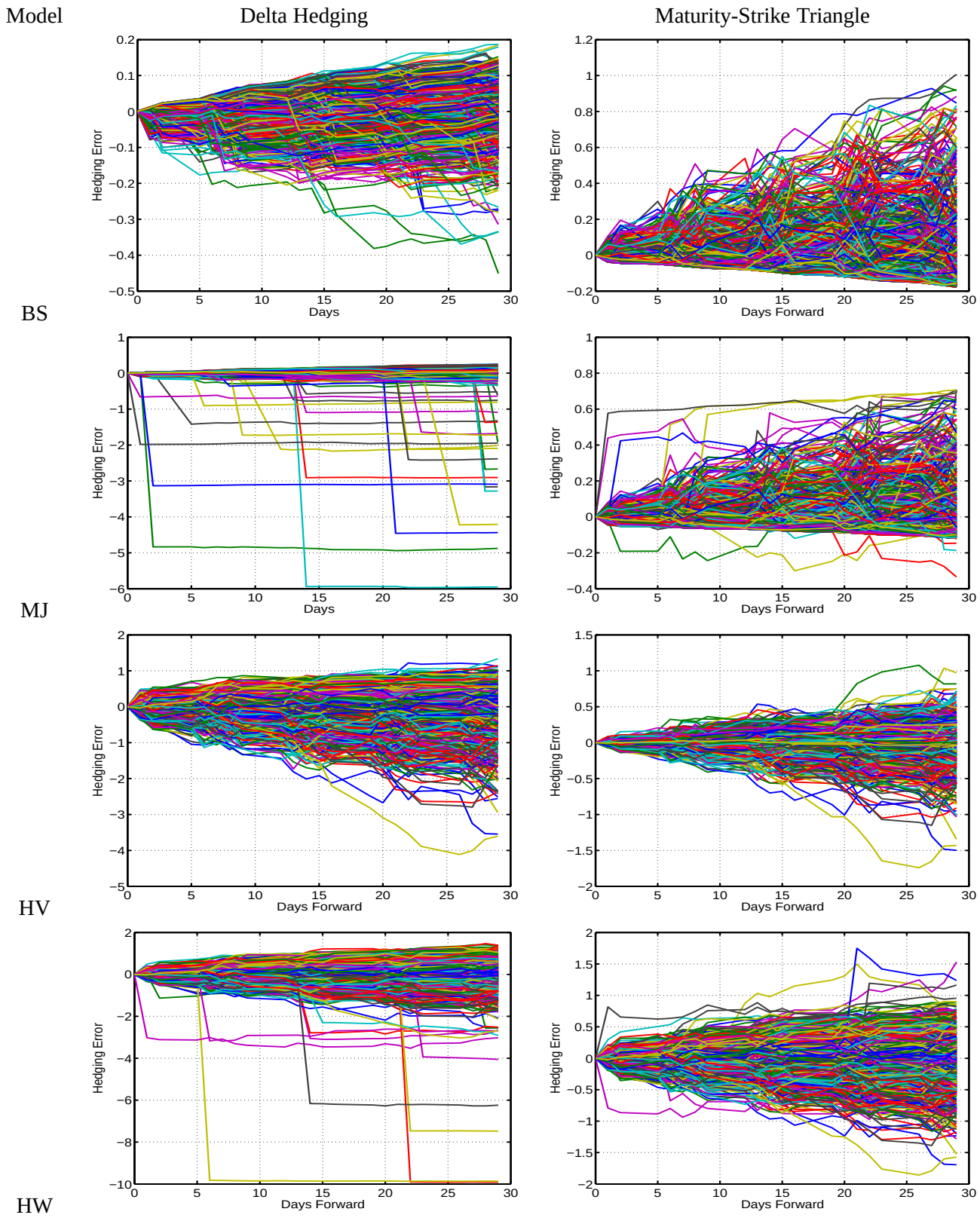

Figure 10. Comparing the simulated sample paths for the hedging errors.
Lines represent the simulated sample paths for the hedging errors under the HW model environment from daily delta hedging with the underlying futures in the left panel and static hedging with the maturity-strike triangle with center strike at one month and outer strikes at two months.

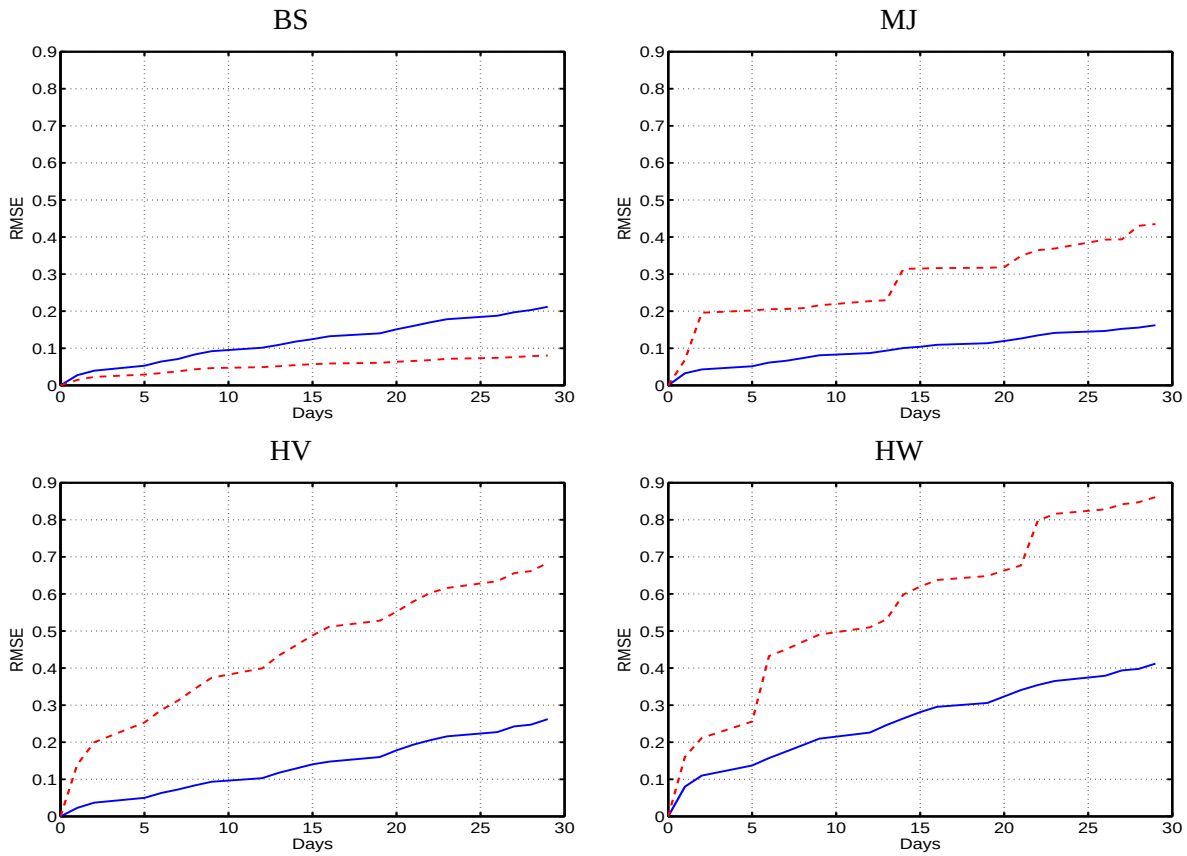

Figure 11. Comparing the cumulation of root mean squared hedging errors over time.
The solid lines denote the RMSE from the maturity-strike triangle hedge at different days forward. The dashed lines denotes the RMSE from daily delta hedge.

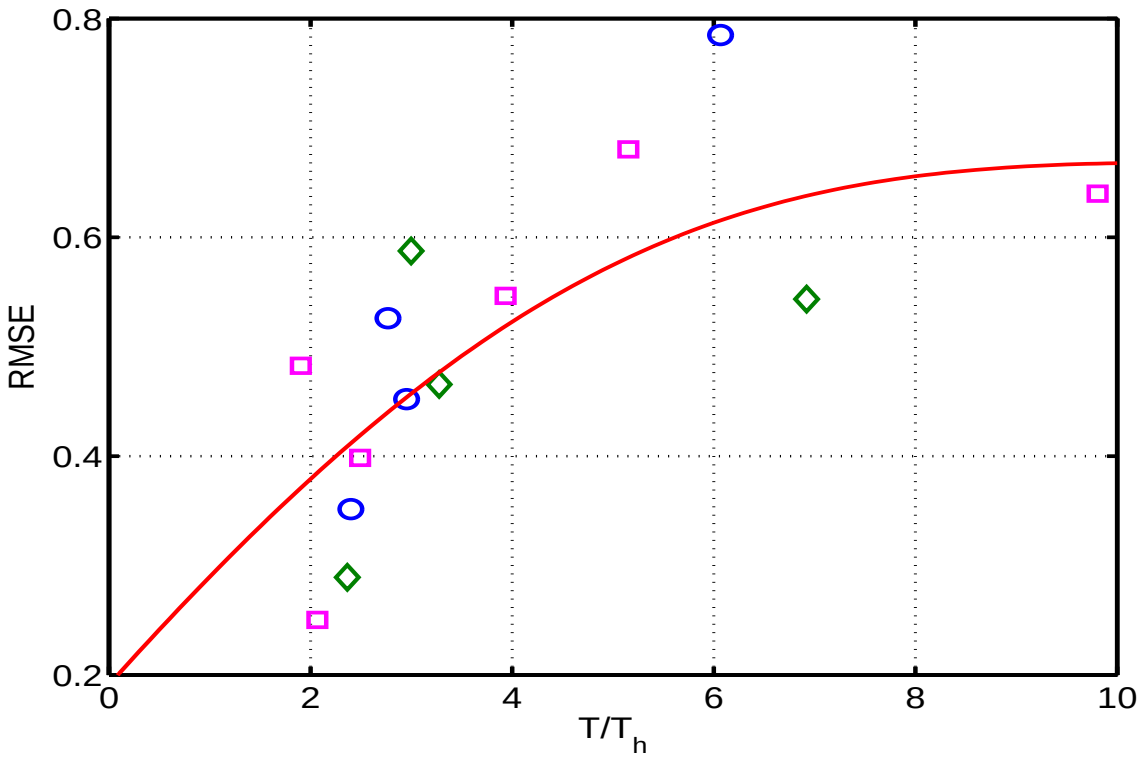

Figure 12. Dependence of hedging performance on target/hedge maturity difference T/T_h.
We measure the maturity distance as the ratio of the target option maturity to the average maturity of options in the hedge portfolio (T/T_h), and we plot the root mean squared hedging error on the SPX options as a function of this maturity ratio. The circles represent maturity-strike triangles with $T_c < T_o < T$; the diamonds represent maturity-strike triangles with $T_o < T_c < T$; and the squares represent the hedge portfolios of three strikes at one maturity $T_h < T$.

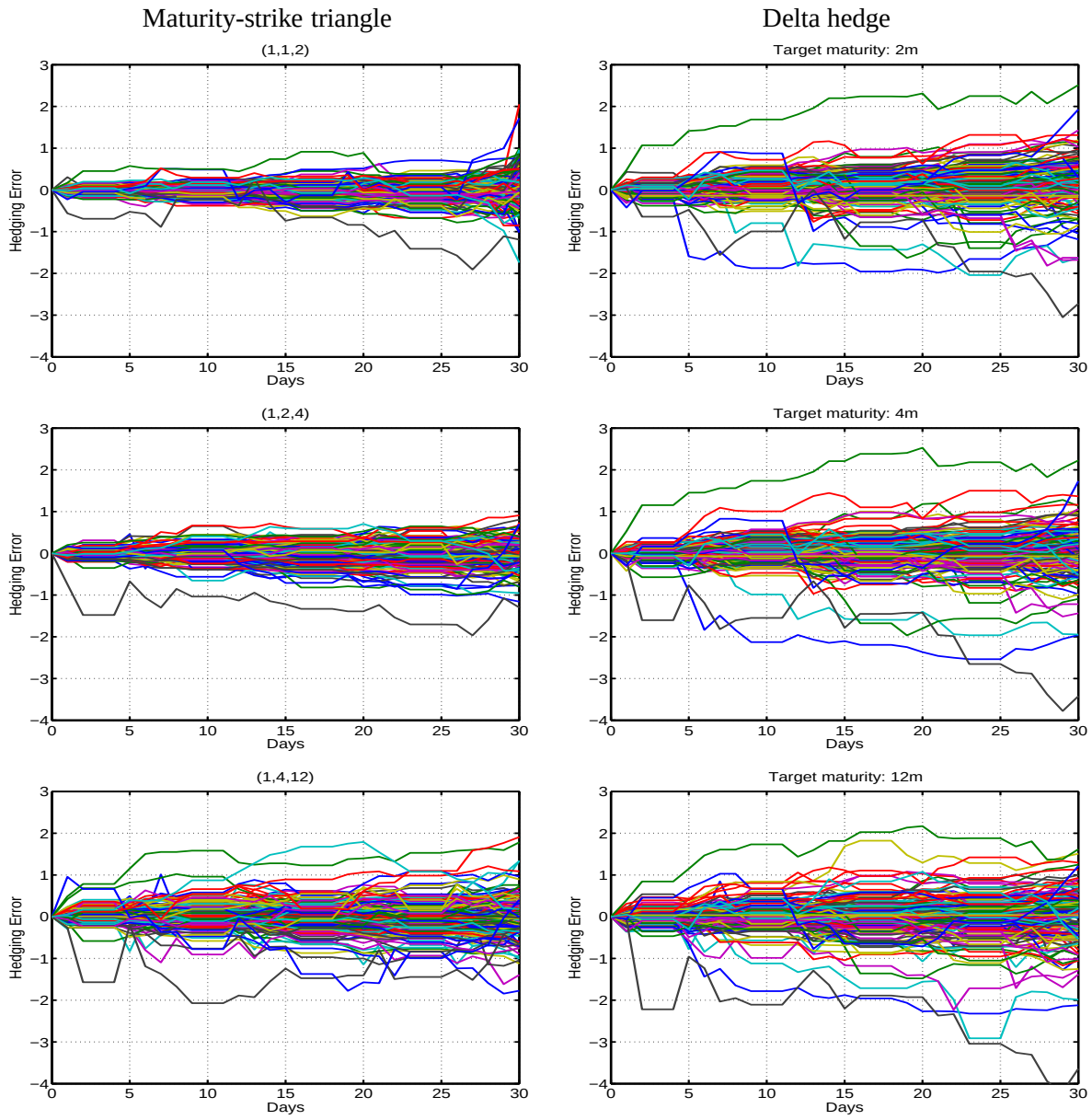

Figure 13. Comparing the hedging error sample paths on S&P 500 index options.
Lines represent the sample paths for the hedging errors on S&P 500 index options from maturity-strike triangles (left side) and delta hedge (right side). The three numbers on top of each panel on the left side represent the three maturities (T_c, T_o, T) for the static portfolios.